

Optoelectronic synapses with chemical-electric behaviors in gallium nitride semiconductors for biorealistic neuromorphic functionality



Open Access This file is licensed under a Creative Commons Attribution 4.0 International License, which permits use, sharing, adaptation, distribution and reproduction in any medium or format, as long as you give appropriate credit to the original author(s) and the source, provide a link to the Creative Commons

license, and indicate if changes were made. In the cases where the authors are anonymous, such as is the case for the reports of anonymous peer reviewers, author attribution should be to 'Anonymous Referee' followed by a clear attribution to the source work. The images or other third party material in this file are included in the article's Creative Commons license, unless indicated otherwise in a credit line to the material. If material is not included in the article's Creative Commons license and your intended use is not permitted by statutory regulation or exceeds the permitted use, you will need to obtain permission directly from the copyright holder. To view a copy of this license, visit

<http://creativecommons.org/licenses/by/4.0/>.

REVIEWER COMMENTS

Reviewer #1 (Remarks to the Author):

The authors reported the multifunctional synaptic characteristic with closed- and open-circuit using conventional pn junctions, which are widely used. The manuscript is well-organized, explaining detailed mechanism analyses and comparative experiments, rather than merely presenting their findings. However, considering the competitive landscape of the field of neuromorphic computing, there seems to be a need for more distinctive novelty in this work. The materials in their manuscript are now commonly reported in terms of both performance and methodology, and the measurement methods are also already well-established for using the electrolytes. Considering these points, the authors should address the following concerns to be published in Nature Communications.

1. The necessity of electrochemical reaction in ion environments is well-known for imitating biological neuron activity. However, the reviewer wonders about a connection between their report and real-biological ion reaction in the human body. In fact, the authors didn't use the major ions (e.g., alkali ions) that are used in biological neuron environment. Describing the use of common metals or protons to mimic biological functions seems to be a lack of relevance and biocompatibility with neural ions. Also, it seems debatable to emphasize the use of ions in this manuscript, as the neural functions can be already implemented without using ions. The reviewer would like this point to be carefully discussed.

2. The benchmarks in the introduction section and Fig S3 should be further supplemented with more objective and quantitative comparison of its performance rather than rough explanation. Please provide more detailed benchmarks of your work with dominant parameters.

3. Generally, p-AlGaIn/n-GaN is a commonly used material. Are there any special reason for using this material compared to other materials? Additional explanation for the fundamental advantages or potentials should be provided.

4. Could the authors explain the reason why using the p-type dominant pn-junction? In other words, why did the authors choose the hole for the majority carrier instead of the electron? Also, the reviewer suggests that the authors provide the comparison results for the case of n-type dominant pn-junction by tuning the composition length of p-AlGaIn/n-GaN with other electrolytes.

5. According to the manuscript, due to the significant difference in charge dissipation between open-circuit and closed-circuit conditions, the difference of their results should become more apparent. However, the tendency of time dependent of PSC and PSV seem similar. It would be better to recommend a quantitative analysis, such as the decay time, between internal photoelectric processes and external electrolyte-mediated chemical-electric processes (e.g., decay time), rather than relying on qualitative explanations.

6. It seems the time range is too short to claim the long-term plasticity of synapses. It would be better to extend the measurement time for their results.

7. Cycle-to-cycle (C-to-C) and device-to-device (D-to-D) variations data should be provided.

8. The reviewer was impressed the the author's demonstration of the reactivity of PSC and PSV through various parameters as shown in Fig 4. Although the results are already excellent, it would be even better to confirm the temperature dependence as an additional factor.

9. Although the authors mentioned a dual-mode function of their device, ultimately, PSC and PSV cannot be used simultaneously as only one of them functions at a time. Along with this point, it would be better to mention the further challenges of their work.

10. As a minor comment, please clarify the positive and negative signs in the main figures and describe the direction of the electric field with arrows. Since multiple reactions occur simultaneously in this manuscript, the reviewer thinks the readers can be easily confused.

Reviewer #2 (Remarks to the Author):

Liu et al. demonstrates a novel photoelectrochemical synaptic device based on p-AlGa_N/n-GaN nanowires. By applying such synaptic device in close- or open-circuit, it can exhibit either short-term or long-term plasticity behavior. While the manuscript is novel and of interest to the community, the following questions should be addressed before it may be granted for publication at Nature Communications.

1. Authors come up with an explanation of the short-term plasticity when the device is applied in close circuit. Extra carriers stimulated by the short laser pulse will flow to both the Pt electrode and end of p-AlGa_N to incorporate in the redox reaction with aqueous electrolyte. As what depicted in Fig. 3d, electrolysis of water is considered as the redox reaction happened in the electrolyte. However, authors don't provide experimental evidence of generating hydrogen and oxygen when redox reaction happens.

2. Authors showcase the concentration of H₂SO₄ in electrolyte can modulate the short-term response of the device, while Na₂SO₄ doesn't significantly affect device's performance. It indicates that proton plays an important role in the redox reaction. Similar to my first question, since authors don't provide evidence of generating hydrogen, it is possible that proton react with the p-AlGa_N. More characterization should be implemented to figure out the details of the redox reaction.

3. As authors predicted, coating of Pt nanoparticles on device can facilitate the reaction through the interface of electrolyte/p-AlGa_N. The negative portion of the PSC when laser pulse is on is obviously enhanced with Pt coating as authors' prediction, however, for the first pulse in Fig. 4e, why can we still get some positive PSC during 10.0 s to ~10.02 s if the reaction happens at the interface is much faster than going through the circuit.

4. Concentration of H₂O₂ is a signal of aging and decline of human's cognitive. However, authors should provide more explanation on why H₂O₂ can suppress device's synaptic behavior. As what I mentioned in my first two questions, authors provide limited explanation on the redox reaction happening between the electrolyte and p-AlGa_N, so that although authors provide many methods of modifying the electrolyte such as adding proton, AA, or H₂O₂ to control device's synaptic behavior, the mechanism still confuses me.

Reviewer #3 (Remarks to the Author):

The authors reported a photoelectrochemical synaptic device based on p-AlGa_N/n-GaN semiconductor nanowires for emulating the chemical-electric synaptic processes. STP and LTP of the device were modulated by switching the closed and open circuits, respectively. The synaptic responses were amplified with the use of Pt nanoparticles onto nanowire surfaces. The optoelectronic synapses were presented to show the modulation by employing the chemical-electric manner. However, before considering its publication, some critical issues need to be addressed.

(1) Many types of material systems, including transition oxide, and van der Waals 2D materials, are developed to electronic or optoelectronic synapses. Why did you use the materials of GaN-based systems? Please give a more detailed explanation.

(2) In recent years, some timely and significant works presented nitride-based materials, such as micro/nanowire, and cantilever-structured GaN, for developing novel memristors or synapses. However, this paper does not cite any reference to the field. Please add such related citations.

(3) Synapse is a kind of ultralow power device for emerging computing architecture. The device shows a reasonably large leakage current level of nA. Could you comment on that?

(4) High-resolution TEM characterization should be provided to represent the crystal structure of AlGa_N/GaN.

(5) Please provide some experimental evidence to illustrate the interplay of optoelectronic and chemical-electric behavior for the GaN-based synapse. And the working mechanism should be talked more about.

(6) The author tested the devices using an electrochemical workstation, and there may be curve drift during testing. Will there be any changes in the performance of the devices?

(7) The photoelectrochemical synapse operated in current mode (STP) or voltage mode (LTP) by altering the circuit state (either closed-circuit or open-circuit). It is confused for synaptic updates when compared to the reported synapses. Could you explain why uses such operations of circuit state?

Response letter

First of all, we would like to express our gratitude and appreciation to the reviewers and editor for the thorough review of our manuscript and the valuable comments and suggestions. We have addressed these comments **point by point** in the following response and **have revised the manuscript accordingly**.

Reviewer #1:

Overall comment: The authors reported the multifunctional synaptic characteristic with closed- and open-circuit using conventional pn junctions, which are widely used. The manuscript is well-organized, explaining detailed mechanism analyses and comparative experiments, rather than merely presenting their findings. However, considering the competitive landscape of the field of neuromorphic computing, there seems to be a need for more distinctive novelty in this work. The materials in their manuscript are now commonly reported in terms of both performance and methodology, and the measurement methods are also already well-established for using the electrolytes. Considering these points, the authors should address the following concerns to be published in Nature Communications.

[Overall response]

Thank you very much for your critical review of our manuscript and your kind feedback to improve the quality of our manuscript. We would like to address your concerns one by one as follows. In regards to your first concern on the novelty of our work, we would like to clarify first: Indeed, the GaN material and the corresponding methodology are commonly employed for constructing semiconductor optoelectronic and power devices. However, there has been very limited research on building GaN-based synaptic devices, especially those operating in the electrolyte environment. Thus far, to the best of our knowledge, there have been no demonstrations of chemically-regulated GaN-based synaptic devices with tunable chemical functionalities. Herein, AlGaIn/GaN nanowires are employed to construct photoelectrochemical synapse with distinctive chemical-electric processes and chemical-related functions. Furthermore, we agree with you that conventional photoelectrochemical devices using electrolytes are well-established; however, their applications have primarily focused on photodetection and biosensing, rather than on synaptic behavior and operation. In this Article, we develop GaN-based photoelectrochemical synapse that offers us new perspective in the pursuit of multifunctional photoelectrochemical device for various applications. Detailed elaboration on the significance and novelty of our work can be found in our response to your Comment 2. Overall, we would like to express our gratitude once again for the careful review and valuable comments.

Comment 1. The necessity of electrochemical reaction in ion environments is well-known for imitating biological neuron activity. However, the reviewer wonders about a connection between their report and real-biological ion reaction in the human body. In fact, the authors didn't use the major ions (e.g., alkali ions) that are used in biological neuron environment. Describing the use of common metals or protons to mimic biological functions seems to be a lack of relevance and biocompatibility with neural ions. Also, it seems debatable to emphasize the use of ions in this manuscript, as the neural functions can be already implemented without using ions. The reviewer would like this point to be carefully discussed.

[Response]

This is really a very good point and we thank you for your valuable insights on ion-associated processes. To address your comments, we primarily focus our discussion from the following three aspects:

A. Importance of ion usage in this work

We fully agree with your comment regarding the necessity of electrochemical reactions in ion environments for imitating biological neuron activity. For electrical synaptic devices, many significant works, which incorporate ion environments and ion-associated processes, have been reported to simulate neuromorphic functions, such as organic electrochemical transistors [*Nat. Rev. Mater.* **9**, 134–149 (2024)] and fluidic memristors [*Nat. Electron.* **7**, 271–278 (2024); *Science* **379**, 156–161 (2023)]. Compared to synaptic devices without ion processes, these devices exhibit unique advantages in the biohybrid field and mimicking chemical neuromorphic functionalities.

Recently, optoelectronic synaptic devices that integrate the photo-electric effect and synaptic plasticity have attracted significant attention, in which synaptic behaviors can be realized through mechanisms such as photogenerated carrier trapping without ion processes [*Nat. Electron.* **5**, 761–773 (2022); *Adv. Funct. Mater.* **32**, 2110976 (2022)]. However, such operation mechanisms without the usage of ions may limit the potential of optoelectronic synapses for diverse tunability and multifunctional applications. Specifically, by introducing an aqueous working environment and ion/molecule-associated processes, new promising applications could be developed: 1) These optoelectronic synapses, operating within ion environments, hold promise for biohybrid applications, as demonstrated in previous studies [*Nat. Mater.* **19**, 969–973 (2020)], thereby facilitating the realization of optical brain-machine interfaces. 2) Furthermore, the incorporation of a chemical environment containing various ions and molecules can endow optoelectronic synapses with chemical-regulated and sensitive capabilities. Such feature not only aids in mimicking biorealistic visual systems with chemical-regulated processes but also offers the potential for multimodal sensing of both visual and chemical cues, thus broadening the application scope of existing optoelectronic synapses. Therefore, it is crucial to develop optoelectronic synapses with ion processes. In our study, we employ a photoelectrochemical configuration to introduce an electrolyte working environment and ion/molecule-related processes within optoelectronic synapses, leading to the demonstration of dual-modal synaptic plasticity and rich chemical-regulated synaptic behaviors.

B. Connection between our study and biological ion reactions

In biological systems, neural information transmission at synapses primarily involves ion-associated and neurotransmitter-associated processes. Ion-associated processes predominantly involve the efflux or influx of Na^+ , K^+ , and Cl^- ions through ion channels, leading to excitatory or inhibitory neuronal activities, while neurotransmitter-associated processes encompass the release, transmission, binding to postsynaptic receptors, and subsequent recycling or degradation of neurotransmitters. Due to the complexity of biological systems and the intrinsic working principles of artificial electronic devices, for artificial devices, it is quite challenging to exactly replicate the species and behaviors of ions and molecules found in biological systems. Although the ion processes and species in these devices differ significantly from those in biological systems, recent studies have exhibited that artificial synaptic devices with ion processes exhibit excellent neuromorphic functionalities and can successfully mimic biorealistic feedback systems. For instance, in organic electrochemical transistors, an electrolyte serves as the gate dielectric. When a gate voltage is applied, ions in the electrolyte penetrate the channel, altering the doping level and conductivity, thereby achieving synaptic function [see the following works as representative: *Nat. Commun.* **13**, 901 (2022); *Nat. Rev. Mater.* **9**, 134–149 (2024)]. In hydrogel-based devices, light or electrical stimuli are employed to facilitate ion movement and release (e.g., azo-benzene functionalized imidazole ions), which modulate ionic conductivity to emulate synaptic function and biological behaviors [*Sci. Adv.* **9**, eadd6950 (2023); *Proc. Natl Acad. Sci. USA* **120**, 2211442120 (2023)]. In our device, ions and molecules in the electrolyte environment (e.g., protons and ascorbic acid) undergo

redox reactions with photogenerated electrons/holes at the electrolyte/semiconductor interface, which shows diverse chemical-regulated synaptic behaviors. In our view, replicating biological ion reactions and mechanisms within synaptic devices is highly significant. This idea has been preliminarily exhibited by recent studies on fluidic memristor [*Science* **379**, 156–161 (2023)], which mimic ion channels and achieve synaptic behavior through hysteretic ion transport, thereby emulating chemical-related functions. However, considering that this field is still in its early stages, the primary focus of recent researches has not been on mimicking real biological ion reactions. Additionally, constructing such systems is quite challenging and requires interdisciplinary collaboration, which will be our goal in future endeavors.

Regarding the relevance of our device to biological systems, we elaborate as follows: 1) While the ion reaction within our device primarily involves protons, the electrolyte environment of our device is PBS solution (physiological electrolyte), which containing Na^+ , K^+ , and Cl^- ions, identical with biological systems. In the future, we will explore the use of Na^+ , K^+ , and Cl^- ions to replace protons to achieve synaptic responses. 2) The semiconductor/electrolyte junction in our device is inspired by the intracellular/extracellular form in biological systems. Based on such configuration, inspired by transmembrane receptors that connect extracellular and intracellular events, synaptic responses can be amplified by applying chemical modifications to nanowire surfaces, which tune external and internal charge behaviors. 3) Furthermore, we add H_2O_2 and ascorbic acid into our device, both of which involve physiological functions in biological systems. These molecules also exert synaptic modulation effects within our device, demonstrating chemically-regulated synaptic activities and oxidative stress-related behaviors induced by increased H_2O_2 concentration similar to those observed in biological systems.

C. Biocompatibility of our device

In our study, phosphate buffered saline (PBS) solution is used as the working environment for the photoelectrochemical synapse, which is a physiological electrolyte and widely used in biological experiments [*Adv. Sci.* **8**, 2001750 (2021)]. GaN and AlGaIn possess excellent biocompatibility and biosafety, which have been used for bone regeneration [*Adv. Funct. Mater.* **31**, 2007487 (2021)]. Moreover, photoelectrochemical devices have been utilized for in vivo biosensing [*Anal. Chem.* **96**, 6079–6088 (2024)]. Overall, both the working environment and materials of our device are biocompatible. And studies on in vivo biosensing with photoelectrochemical devices have been reported, thus suggesting that the photoelectrochemical synapse is promising for constructing biohybrid systems. Currently, we have achieved glucose levels detection in human serum using a photoelectrochemical device [*Nano-Micro Lett.* **16**, 192 (2024)]. In our future work, we aim to realize a closed-loop neuromorphic systems which involve the interactive communications between the photoelectrochemical synapse and biological cells.

To address your concern, in the revised Supplementary Information, we have incorporated the above discussion and description, and add new content in the revised manuscript.

In the revised manuscript, we have added following content:

Furthermore, the aqueous electrolyte environment containing ions and molecules is crucial in the construction of the photoelectrochemical synapse. More details on the importance of ion use can be found in Supplementary Note 3.

Additional discussions on the biocompatibility of the device and its relevance to biological systems can be found in Supplementary Note 3.

In the revised Supplementary Information, we have included above discussions in Supplementary Note 3. The importance of ion use, device biocompatibility, and its relevance to biological systems.

Comment 2. The benchmarks in the introduction section and Fig S3 should be further supplemented with more objective and quantitative comparison of its performance rather than rough explanation. Please provide more detailed benchmarks of your work with dominant parameters.

[Response]

We appreciate your valuable comments on device performance comparison and description. Below is our detailed quantitative analysis: In current mode, the device exhibits PPF index of 217% and synaptic behavior lasting for approximately 60 s, demonstrating short-term plasticity. In voltage mode, the device shows PPF index of 293% and synaptic behavior lasting for over 1500 s, indicating long-term plasticity. After Pt nanoparticle decoration, the synaptic responses are significantly enhanced, with the current response doubling and the voltage response slightly increasing. We have added objective and quantitative performance comparisons in the third paragraph of the introduction section. Additionally, to objectively illustrate the device performance, we have also supplemented quantitative performance comparisons and descriptions in the results section. Details are listed at the end of this response.

In Figure S3, we discuss the mechanisms of different types of semiconductor-based synaptic devices, highlighting the distinctions in working principles between our device and previous ones. To enhance clarity and readability, we present a summary of the mechanisms of different devices in **Table R1**. For synaptic devices, besides the neuromorphic computing field, many studies focus on the bionic functionalities and applications, which is also the focus of our work. To illustrate the differences between our device and previous works, as well as the novelty of our study, we have conducted a detailed discussion. Specifically, we analyzed and compared our work with previous studies in three aspects, primarily focusing on device structures and their functional applications.

A. Comparing with previous neuromorphic devices with electrolyte-mediated processes

Previous neuromorphic devices with electrolyte-mediated processes, such as organic electrochemical transistors, fluidic memristors, and other novel devices, are typically employed for developing electrical synapses, optoelectronic synapses, and the incorporation of chemical-electric processes into electrical synapses, as summarized in **Table R2**. In contrast, our proposed synaptic device, based on photoelectrochemical structure, manifests distinctive dual-modal synaptic plasticity and rich chemical-related functionalities through the interplay of photo-electric and chemical-electric synaptic processes, providing a novel platform for the advancement of multifunctional optoelectronic synapses.

B. Comparing with previous GaN-based synapses

We compare our work with previously reported GaN-based synaptic devices (**Table R3**). As you may notice, previously reported GaN-based synaptic devices typically employ either transistor structure with three terminals or electrode-semiconductor-electrode structure with two terminals, leveraging the photoelectric or piezoelectric effect of GaN to construct optoelectronic synapses or strain-sensitive electrical synapses, which do not involve chemical regulation process. In contrast, we propose a synaptic architecture based on photoelectrochemical structure and incorporate chemical-electric processes into optoelectronic synapse, leading to the demonstration of dual-modal plasticity and rich chemical-related functions, offering expanded applications for GaN materials in the field of constructing optoelectronic synapse.

C. Comparing with previous photoelectrochemical devices

Photoelectrochemical devices have been widely investigated but primarily utilized for photodetection and biosensing. Recent developments in photodetection involve photodetectors with multi-wavelength discrimination capability, which have been applied in optical communication and logic gates [*Nat. Electron.* **4**, 645–652 (2021); *Adv. Mater.* **36**, 2307779 (2024)]. In the field of biosensing, the

photoelectrochemical strategy exhibits high sensitivity and low background noise, facilitating the detection of various biological substance such as DNA and tumor markers [*Anal. Chem.* **92**, 363–377 (2020)]. However, the potential application of photoelectrochemical structure in neuromorphic devices remains largely unexplored. The photoelectrochemical architecture allows for the introduction of chemical-electric processes into optoelectronic synapses, thus expanding their potential application. Moreover, in our future work, we aim to further enhance the device functionalities and applications of photoelectrochemical synapses by leveraging the well-established photoelectrochemical applications including multi-wavelength detection and biosensing.

To provide an objective and quantitative description of the device performance, the following content has been added to the revised manuscript (the supplemented contents are highlighted in red):

1. In current mode, the device exhibits PPF index of 217% and synaptic behavior lasting for approximately 60 s, whereas in voltage mode, it shows PPF index of 293% and synaptic behavior lasting for over 1500 s.

2. Furthermore, inspired by the transmembrane receptors in biological synapses, chemical modification (e.g., Pt nanoparticle decoration) was introduced to the semiconductor surface, which effectively modulated external charge consumption and internal charge transport, leading to amplified synaptic responses with the current response doubling and the voltage response slightly increasing.

3. The Δ PSC gradually decays to the original state after stimulation and the synaptic response lasts for approximately 60 s (Supplementary Figure 7)

4. the device shows the maximum PPF index of 217% and the PPF index decreases as the time interval between the two pulses increases.

5. The test with extended measurement time is depicted in Supplementary Figure 14, with synaptic response lasting for over 1500 s in voltage mode.

6. The device shows the maximum PPF index of 293% and the PPF curve is well fitted using a double exponential decay function (Fig. 2e(ii))

7. while the negative current is significantly boosted, reaching twice that of the pristine device (Fig. 4e).

In the revised Supplementary Information, to highlight the distinction between our work and previously reported studies, we have included the above discussions and all tables in Supplementary Note 2. Comparison of working principles and device functionalities with previous studies.

Table R1. Comparison of different types of semiconductor-based synapses

Device type	Device configuration	Electrolyte compatibility	Operation mechanism
Solid-state synapse	Two or three-terminal	No	Diverse working mechanisms
Electric-double-layer transistor (EDLT)	Three-terminal	Yes	Interface electric-double-layer capacitor modulation
Organic electrochemical transistor (OECT)	Three-terminal	Yes	Ion penetration induced semiconductor doping
Photoelectrochemical synapse	Two-terminal	Yes	Interface redox reaction and internal photoexcited carrier accumulation

Table R2. Comparison of various electrolyte-mediated neuromorphic devices

Materials	Device type	Stimuli	Functionalities and applications	Ref.
PimB-Confined Channel	Fluidic memristor	Electrical, chemical	Chemical-regulated plasticity, chemical-electric signal transduction	<i>Science</i> 379 , 156-161 (2023)
n-type OMIEC	OECT	Electrical, chemical	ANN simulation, dopamine neuromorphic sensing	<i>Angew. Chem. Int. Ed.</i> 136 , 202315537 (2024)
Azo-tz-PEDOT:PSS	OPECT	Light, electrical	Visual pathway mimicking, optoelectronic synaptic memory	<i>Nat. Commun.</i> 14 , 6760 (2023)
Fiber PEDOT:PSS	OECT	Electrical, chemical	Dopamine-dependent plasticity	<i>Adv. Mater.</i> 36 , 2305371 (2024)
PEDOT:PSS	OECT	Electrical, chemical	Selective plasticity modulation by glucose	<i>Angew. Chem. Int. Ed.</i> 62 , 202302723 (2023)
PEDOT:PSS	OECT	Electrical, chemical	Dopamine-mediated plasticity, biohybrid synapse	<i>Nat. Mater.</i> 19 , 969–973 (2020)
Hydrogel	Ionic diode	Electrical	Dendritic signal integration	<i>Proc. Natl Acad. Sci. USA</i> 120 , 2211442120 (2023)
Graphene and CaF ₂	Chemimemristor	Electrical	Long-term memory	<i>Proc. Natl Acad. Sci. USA</i> 121 , 2314347121 (2024)
p-AlGaIn/n-GaN	Photoelectrochemical	Light, electrical, chemical	Dual-modal synaptic plasticity, surface chemical modification, chemical-regulated behavior	This work

OMIEC, organic mixed ionic-electronic conductors; OECT, Organic electrochemical transistor; ANN, artificial neural network; Azo-tz-PEDOT:PSS, poly(3,4-ethylenedioxythiophene) polystyrene sulfonate (PEDOT:PSS) covalently bonded to azobenzenes moieties; OPECT, organic photoelectrochemical transistors;

Table R3. Comparison between previous GaN-based synapses and photoelectrochemical synapse

Materials	Device structure	Stimuli	Functionality and application	Ref.
Perovskite-gated AlGaIn/GaN	HEMT	Light, electrical	Gate-tunable synaptic behaviors, retinal cell simulation, image preprocessing and classification	<i>Adv. Sci.</i> 9 , 2202019 (2022)

AlGaIn/GaN heterojunction	HEMT	Light, electrical	Optoelectronic logic gate	<i>Adv. Optical Mater.</i> 11 , 2202105 (2023)
Si-doped GaN film	MSM	Light, electrical	Learning-experience behavior, visual recognition and memorization	<i>J. Mater. Chem. C</i> 10 , 13099 (2022)
GaN/AlN periodic structure	MSM	Light, electrical	Image information preprocessing	<i>ACS Appl. Nano Mater.</i> 6 , 8461–8467 (2023)
(Al,Ga)N nanowire	MSM	Light, electrical	Handwritten image recognition	<i>Nano Res.</i> 17 , 1933-1941 (2024)
GaN nanowire	MSM	Light, electrical	Learning-experience behavior, handwritten image recognition	<i>Photonics Res.</i> 11 , 1667-1677 (2023)
AlGaIn/GaN	HEMT	Light, electrical	Dual-synapse integration, letter recognition and classification	<i>Nano Energy</i> 125 , 109564 (2024)
GaN microwire	MSM	Strain, electrical	Threshold switching behavior, short-term plasticity, piezotronic modulated plasticity	<i>Nano Lett.</i> 20 , 3761–3768 (2020)
GaN nanowire	MSM	Electrical	Nonvolatile memristive behaviors, short-term plasticity	<i>Adv. Funct. Mater.</i> 33 , 2306030 (2023)
GaN Microwire	MSM	Strain, electrical	Multilevel switching capability, piezotronic modulated behaviors	<i>Adv. Funct. Mater.</i> 26 , 5307–5314 (2016)
GaN Microwire	MSM	Strain, electrical	Strain sensing and memorizing, haptic memory array	<i>Nano Energy</i> 78 , 105312 (2020)
p-AlGaIn/n-GaN nanowire	Photoelectrochemical	Light, electrical, chemical	Dual-modal synaptic plasticity, surface chemical modification, visual memorization, chemical-regulated behaviors	This work

HEMT, High-Electron-Mobility Transistor; MSM, metal-semiconductor-metal structure with two terminals

Comment 3. Generally, p-AlGaIn/n-GaN is a commonly used material. Are there any special reason for using this material compared to other materials? Additional explanation for the fundamental advantages or potentials should be provided.

[Response]

We appreciate your insightful comments on the material choice. In our study, we employ p-AlGaIn/n-GaN nanowires due to their exceptional optoelectronic characteristic and chemical properties, as well as their promising scalability for future development. The detailed rationale is outlined below:

(1) Excellent optoelectronic characteristics: GaN is a direct bandgap semiconductor material, making it suitable for fabricating optoelectronic devices. When they are grown by plasma-assisted molecular beam epitaxy (MBE), GaN nanowires exhibit high crystallinity and large surface-to-volume ratio, giving rise to superior light absorption and charge carrier behaviors, rendering them as great material candidates in building optoelectronic devices [*Nat. Electron.* **4**, 645–652 (2021); *Adv. Mater.* **36**, 2307779 (2024)].

(2) Superior material for chemical-related applications: GaN material demonstrates chemical stability in aqueous solutions, thereby widely applied in studies involving electrolyte-mediated chemical reactions [*Nature* **613**, 66–70 (2023)]. Furthermore, the one-dimensional structure of nanowires provides a large surface area, making them highly sensitive to electrolyte solutions and thus ideal for constructing synaptic devices with chemical-related functionalities. The photoelectrochemical synapse leverages the interplay of photo-electric and chemical-electric processes to achieve various synaptic functions. GaN materials exhibit excellent performance in optoelectronic and chemical-related device applications, making them an ideal choice for our photoelectrochemical synapse.

(3) Controllable material growth and promising scalability: The growth of GaN material is highly controllable with the epitaxy techniques such as MBE or metal organic chemical vapor deposition (MOCVD) enabling precise control over alloy composition (e.g., AlGa_N or InGa_N) and doping concentration. This controllable growth processes enhances the scalability of GaN materials. By regulating the alloy composition in GaN, the bandgap can be tuned, allowing the material system to cover a broad spectrum ranging from the ultraviolet to the near-infrared [*Nat. Mater.* **6**, 951–956 (2007)]. This capability facilitates future research on optoelectronic synapses with a broad spectral response.

(4) Potential integration with other device: Notably, GaN-based systems have been widely used in developing optoelectronic devices (e.g., photodetector, LED), electronic devices (e.g., high-electron-mobility transistor, Schottky barrier diode), and piezoelectric pressure sensors. Through rational device structure design and advanced micro-nano fabrication processes, our device could be integrated with these devices. Additionally, the GaN nanowires used in our device are based on a CMOS-compatible and low-cost silicon platform, highlighting its great promise in future integrated Si-photonics applications.

In the revised manuscript, we have included the clarification of the advantages of GaN-based nanowires: GaN materials exhibit excellent optoelectronic and piezoelectric properties^{21,26}. In recent years, there have been notable works utilizing GaN materials, including micro/nanowires and cantilever structures, for the development of strain-sensitive electrical synapses²⁶⁻³⁰ and optoelectronic synapses^{31,32}. GaN materials demonstrate good chemical stability in electrolyte solution, making it suitable for researches involving electrolyte-mediated chemical reactions³³. Furthermore, GaN materials exhibit tunable bandgap and show promising prospects for device integration³⁴. During epitaxial growth, the bandgap of GaN materials can be controlled by adjusting the alloy composition (e.g., AlGa_N or InGa_N), enabling the material system to cover a broad spectrum from ultraviolet to near-infrared³⁴. More importantly, GaN-based nanowires, characterized by outstanding crystallinity and large surface-to-volume ratio, are particularly attractive in optoelectronic applications due to their superior light absorption and charge carrier behaviors^{33,35}. Additionally, in an aqueous environment, the large surface area of the one-dimensional structure makes the nanowires exceptionally sensitive to electrolyte solutions^{36,37}, ideal for constructing optoelectronic synapses with chemical-related functions.

Comment 4. Could the authors explain the reason why using the p-type dominant pn-junction? In other words, why did the authors choose the hole for the majority carrier instead of the electron? Also, the reviewer suggests that the authors provide the comparison results for the case of n-type dominant pn-

junction by tuning the composition length of p-AlGaIn/n-GaN with other electrolytes.

[Response]

We greatly appreciate your insightful comments on band structure design. Essentially, the choice of p-type dominant p-n junction is determined by the functionality we aim to achieve. In our device, our main goal is to construct two back-to-back built-in electric fields to realize charge carrier storage in closed-circuit mode. Therefore, in our device, in addition to the electrolyte/semiconductor junction, we need to use the p-n junction.

A. Rational control of the p-n junction length:

Per your suggestions, we additionally prepared p-n junction nanowires, maintaining the length of p-AlGaIn while increasing the length of n-GaN segment to 200 nm. The test results are depicted in **Figure R1a** and **b**. It is observed that compared to nanowires with 20 nm n-GaN segment, increasing the length of n-GaN substantially enhances the positive current peak in PSC mode. Correspondingly, in PSV mode, it leads to significantly large negative voltage peaks, resulting in unclear curve shapes that are difficult to distinguish. This is because, under illumination, both the p-AlGaIn and the 200 nm n-GaN segment absorb light, leading to more electrons flowing to the semiconductor, thereby resulting in significant peaks and unclear results.

Overall, increasing the length of n-GaN complicates the behavior of charge carriers, resulting in significant peaks and unclear curves, which might not be suitable for our application. In our work, besides introducing two back-to-back built-in electric fields (i.e., p-n junction) to achieve carrier storage, we need to rationally control the length of the p-n junction to regulate synaptic behaviors. This is why we chose the p-AlGaIn dominant p-n junction to store holes for synaptic responses.

B. Changing the electrolyte environment:

As suggested by the reviewer, we replaced the PBS solution with 0.5 M H₂SO₄ for comparative experiments. The results are shown in **Figures R1c** and **d**. In comparison to the synaptic response in PBS solution, in 0.5 M H₂SO₄, the negative current of the device increases, while the negative peak in PSV mode decreases. This is attributed to the increase in proton concentration, accelerating the electron consumption at the semiconductor/electrolyte interface and facilitating electron flow into the electrolyte solution. In PSC mode, during the first light pulse, the slight increase of positive current peak may be due to the higher conductivity of the 0.5 M H₂SO₄ solution compared to PBS solution, leading to accelerated hole consumption and consequently an increase in the positive current peak. It can be concluded that, besides controlling the nanowire structure, altering the electrolyte environment can also regulate the synaptic responses of the device.

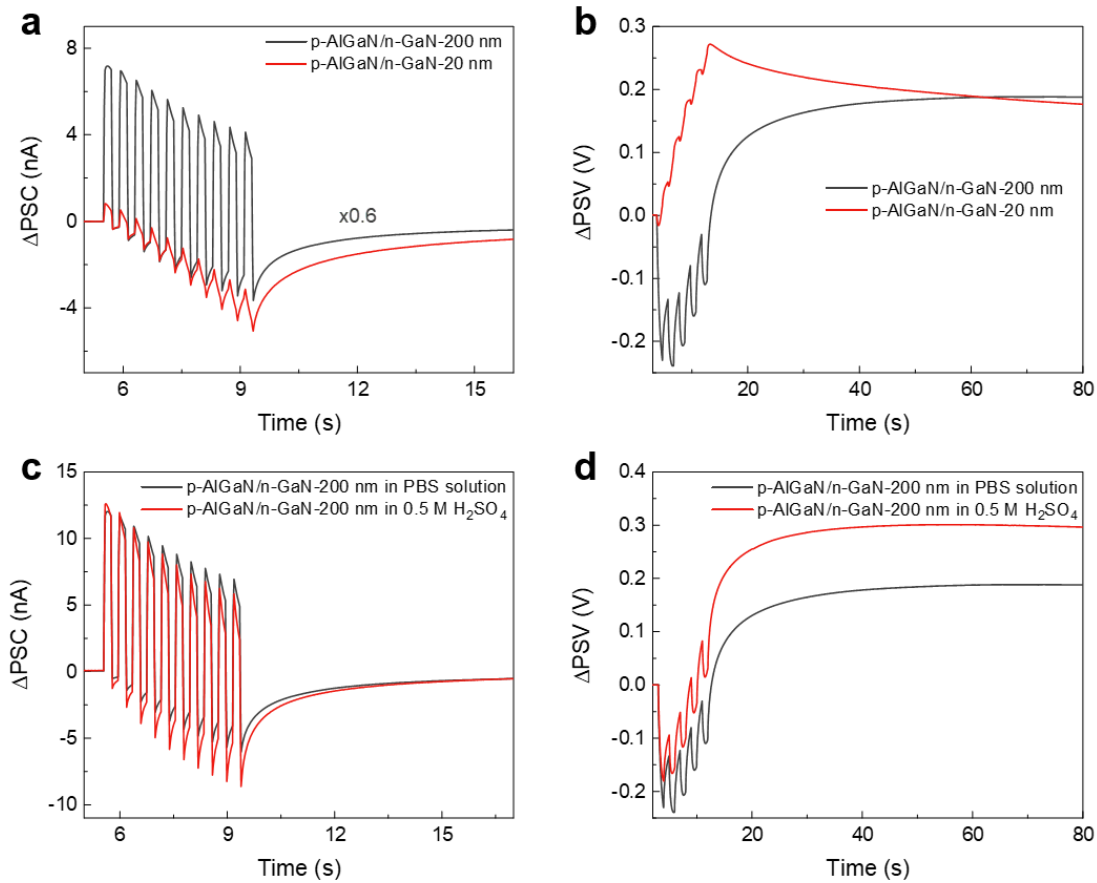


Figure R1. (a, b) Postsynaptic current (a) and postsynaptic voltage (b) responses with different lengths of GaN segment (All tests conducted in PBS solution). (c, d) Synaptic responses of nanowires with a 200 nm GaN segment in PBS solution and 0.5 M H₂SO₄. Light pulses of 255 nm and 12 μW cm⁻² were used.

We have included the above discussion on the investigation of synaptic behavior with different length of p-n junction in the revised manuscript and Supplementary Information.

In the revised manuscript: Furthermore, to illustrate the necessity of controlling the length of p-n nanowire, we prepared additional p-n junction nanowires by maintaining the length of the p-AlGaIn while increasing the length of the n-GaN to 200 nm. The test results are shown in Supplementary Figure 6. It is observed that compared to nanowires with a 20 nm n-GaN segment, increasing the length of n-GaN substantially enhances the positive current peak in current mode. Correspondingly, in voltage mode, this leads to significantly large negative voltage peaks, resulting in unclear curve shapes and difficulty in discerning synaptic behavior. Therefore, in our device, besides introducing p-n junction to achieve carrier storage, we also need to rationally control the length of the p- and n- segment in the p-n junction to control synaptic behaviors.

In the revised Supplementary Information: Supplementary Note 4. Working mechanism validation based on other nanowire samples and device structure.

Comment 5. According to the manuscript, due to the significant difference in charge dissipation between open-circuit and closed-circuit conditions, the difference of their results should become more apparent. However, the tendency of time dependent of PSC and PSV seem similar. It would be better to recommend a quantitative analysis, such as the decay time, between internal photoelectric processes and external

electrolyte-mediated chemical-electric processes (e.g., decay time), rather than relying on qualitative explanations.

[Response]

Thank you for valuable comments on the synaptic behaviors observed in the two modes. Under open-circuit and closed-circuit conditions, the mechanisms of charge carrier accumulation and dissipation exhibit significant differences, with the relaxation process notably slower in PSV compared to PSC. To better illustrate the distinctions between the two modes, we normalize the responses of PSC and PSV, as depicted in **Figure R2**. It can be observed that the relaxation processes of PSC and PSV are obviously different, which are attributed to the distinctive working mechanisms of the two modes.

Regarding the quantitative analysis of photo-electric and chemical-electric processes, our discussion is as follows:

A. Time constants of photo-electric and chemical-electric processes

1) The internal photo-electric processes mainly involve the transfer of photogenerated electrons towards electrolyte or external circuit, as well as the storage and dissipation of photogenerated holes. The transfer of electrons within the semiconductor occurs in the time range of $\sim 10^{-9}$ s [*ACS Nano* **12**, 11088 (2018)], whereas hole dissipation requires much longer time due to the interface barrier, which take at least $\sim 10^2$ s to decay to the initial state [*Adv. Optical Mater.* **11**, 2300317 (2023)].

2) The external electrolyte-mediated chemical-electric processes involve the dissipation of electrons and holes by the electrolyte with the time scale of $\sim 10^{-3}$ s [*ACS Nano* **12**, 11088 (2018)]. Note that these time constants are provided for reference only. Considering our device operates in aqueous environment, the photo-electric and chemical-electric processes are closely connected, making it challenging to measure the specific time required for above two processes. In future work, we will attempt to conduct in-situ time-resolved analyses to study the time-resolved charge carrier dynamics of the distinctive synaptic behaviors.

B. Detailed analysis in our device from illumination to dark conditions

Upon illumination, photogenerated electrons flow towards the electrolyte and external circuit. Owing to the slower transfer and consumption processes of electrons at the electrolyte interface ($\sim 10^{-3}$ s) compared to transfer processes within the semiconductor ($\sim 10^{-9}$ s), photogenerated electrons inevitably flow towards the external circuit first, leading to the initial spike observed in the curve. Upon cessation of illumination, stored holes dissipate slowly ($\sim 10^2$ s), which is much longer than the time required for electron transfer and chemical reactions in the electrolyte ($\sim 10^{-3}$ s). Hence, the recorded curves exhibit a slow relaxation over time. Moreover, in PSC mode, charge carriers can be consumed through both internal circuit and external electrolyte pathways, while the carriers in PSV mode can only dissipate through the external solution, leading to different time dependencies between the two modes (**Figure R2**).

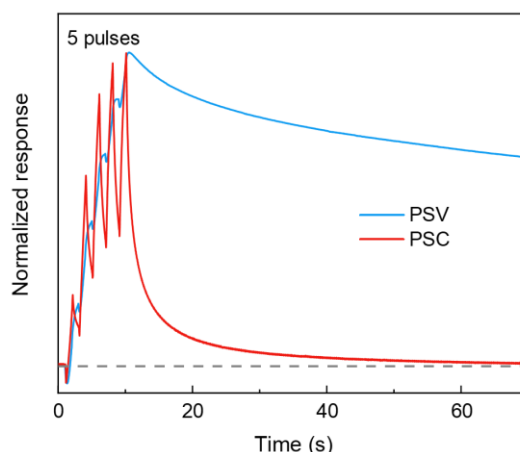


Figure R2. Normalized synaptic responses in the two modes. The same optical stimulation was utilized, with both pulse duration and interval set to 1 s. Light pulses of 255 nm and $12 \mu\text{W cm}^{-2}$ were used.

In the revised manuscript, we have added the following content to illustrate the different time-dependent trends in the two working modes:

To illustrate the differences in the time-dependent trend of synaptic response in both modes, we normalize the postsynaptic current and voltage, as shown in Supplementary Figure 7. After light pulses, the relaxation processes of the device in current mode and voltage mode are obviously different, with the postsynaptic current decaying rapidly while the postsynaptic voltage decays slowly.

The quantitative comparison of the photo-electric and chemical-electric processes can be found in Supplementary Note 5.

In the revised Supplementary Information, we have added Figure R2 and above quantitative analysis of photo-electric and chemical-electric processes: Supplementary Note 5. The quantitative comparison of the photo-electric and chemical-electric processes

Comment 6. It seems the time range is too short to claim the long-term plasticity of synapses. It would be better to extend the measurement time for their results.

[Response]

Thanks for your valuable suggestion. We extend the measurement time to demonstrate the long-term plasticity of our device in voltage mode, as illustrated in **Figure R3**.

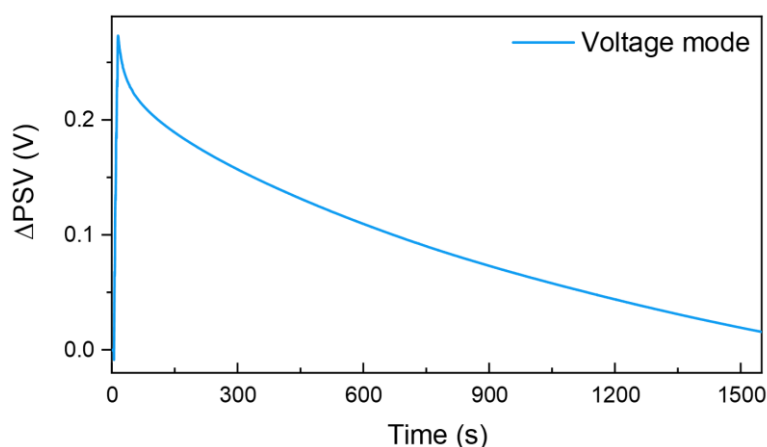


Figure R3. Postsynaptic voltage response of pristine nanowires. Five optical pulses were applied, with both duration and interval set to 1 s. Light pulses of 255 nm and $12 \mu\text{W cm}^{-2}$ were used.

To address your concern, in the revised manuscript, we have added the following content: **The test with extended measurement time is depicted in Supplementary Figure 14, with synaptic response lasting for over 1500 s in voltage mode.**

In the revised Supplementary Information, we have added Figure R3: Supplementary Figure 14

Comment 7. Cycle-to-cycle (C-to-C) and device-to-device (D-to-D) variations data should be provided.

[Response]

Thank you for the useful suggestions. We conducted additional tests to assess cycle-to-cycle and device-to-device variations of the photoelectrochemical synapses in voltage and current modes. In current mode, we compared the peak values after 10 pulses, while in voltage mode, we compared the peak values after 5 pulses. All test results are summarized in **Figure R4**. Here, the variation is defined as the ratio of the standard deviation to the mean. For cycle-to-cycle variation, we tested 30 cycles. In voltage mode, the variation is 1.54%, whereas it is 3.08% in current mode. During the long-term testing, a slight performance decline is observed. To enhance the long-term stability, protective coatings can be employed on the nanowire surface in future work. Regarding device-to-device variation, we prepared 10 devices. In voltage mode, the variation is 3.29%, and it is 3.04% in current mode. In future research, we can further enhance device uniformity by utilizing selective area growth to improve nanowire uniformity.

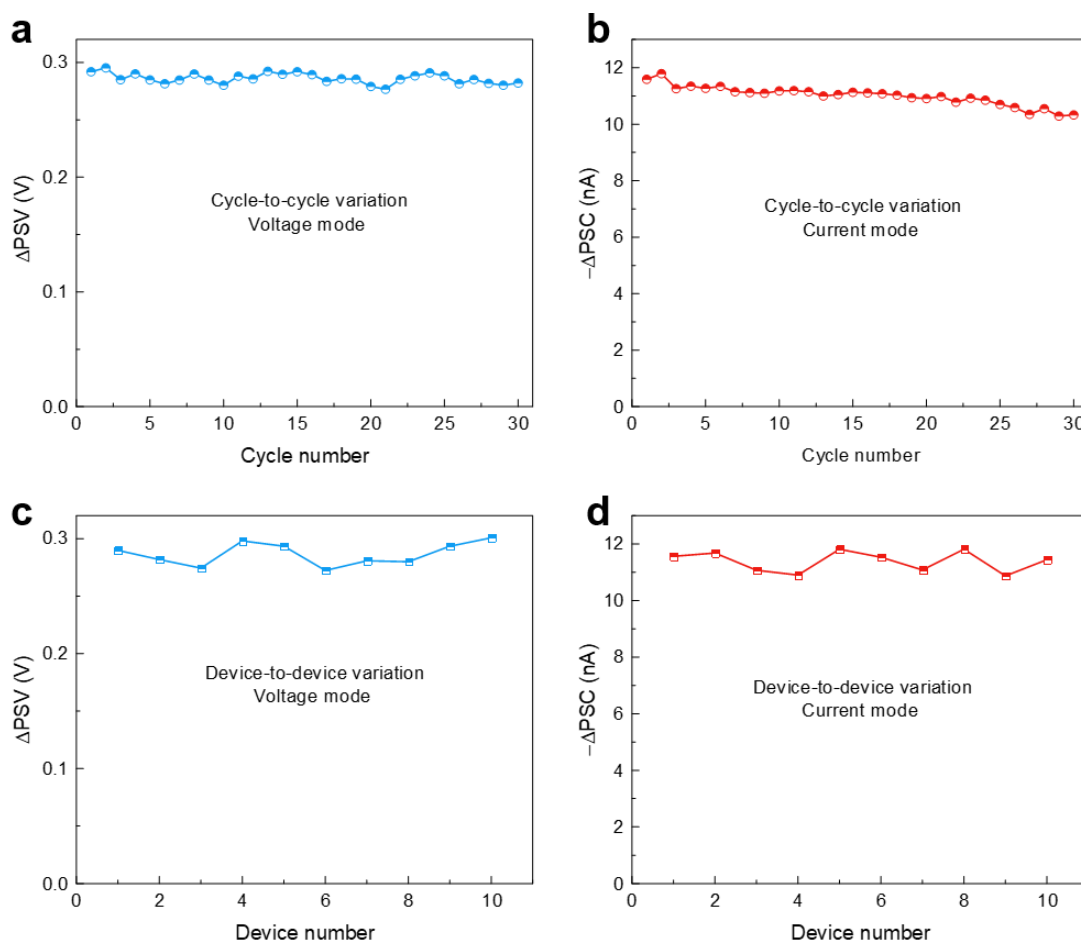


Figure R4. Cycle-to-cycle and device-to-device variation of the photoelectrochemical synapse. (a, b) Cycle-to-cycle variation in voltage mode (a) and current mode (b). (c, d) Device-to-device variation in voltage mode (c) and current mode (d). In current mode, 10 pulses of optical stimulation were utilized, with both duration and interval set to 0.2 s. In voltage mode, 5 pulses of optical stimulation were utilized,

with both duration and interval set to 1 s. We compared the peak values after light stimuli to investigate the variations. Light pulses of 255 nm and $12 \mu\text{W cm}^{-2}$ were used.

In the revised manuscript, we have added the following content to illustrate the cycle-to-cycle and device-to-device variations: The cycle-to-cycle and device-to-device variations of the Pt-decorated synaptic device are summarized in Supplementary Figure 8. In current mode, we compared the peak values after 10 pulses, while in voltage mode, we compared the peak values after 5 pulses. The variation is defined as the ratio of the standard deviation to the mean. For cycle-to-cycle variation, we tested 30 cycles. In voltage mode, the variation is 1.54%, whereas it is 3.08% in current mode. Regarding device-to-device variation, we prepared 10 devices. In voltage mode, the variation is 3.29%, and it is 3.04% in current mode.

In the revised Supplementary Information, we have added Figure R4 and related description: Supplementary Note 6. Cycle-to-cycle and device-to-device variations

Comment 8. The reviewer was impressed the the author's demonstration of the reactivity of PSC and PSV through various parameters as shown in Fig 4. Although the results are already excellent, it would be even better to confirm the temperature dependence as an additional factor.

[Response]

Thanks for your invaluable suggestion. Understanding how temperature influences synaptic device performance is crucial for applications in neuromorphic computing and biomimetic sensing. To address this, we conducted tests of our device at varying electrolyte temperatures, as depicted in **Figure R5**. It can be observed the photoelectrochemical synaptic device exhibits notable temperature-dependent behavior, wherein higher electrolyte temperatures correspond to enhanced synaptic response. This behavior can be attributed to the temperature sensitivity of both the photo-electric and chemical-electric processes, with higher temperatures accelerating chemical reactions at the electrolyte/semiconductor interface and giving rise to larger current [*Adv. Mater.* **33**, 2004406 (2021)]. Moreover, a temperature increase within a certain range can enhance the photoresponse of photodetectors. [*Appl. Phys. Lett.* **120**, 091103 (2022)]. Benefiting from the temperature-dependent synaptic behavior, we anticipate exploring more biorealistic synaptic applications in future research.

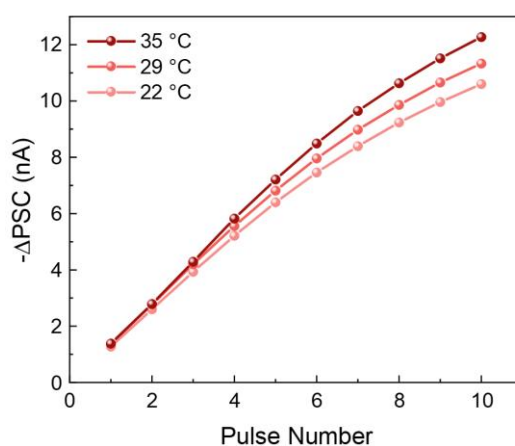


Figure R5. Synaptic response of the photoelectrochemical synapse at different electrolyte temperatures. Note that we take the absolute value of the postsynaptic current ($-\Delta\text{PSC}$) for performance comparison.

In the revised manuscript, we have added the following content to illustrate the temperature-dependent

behavior of our device: In addition to chemical regulation effect, temperature also affects learning and memory behaviors in biological systems. In the photoelectrochemical synapse, the synaptic responses in PBS solution at different temperatures were investigated, as shown in Supplementary Figure 17. As the electrolyte temperature increases, the Δ PSC response significantly increases. This behavior can be attributed to the temperature sensitivity of both the photo-electric and chemical-electric processes, with higher temperature accelerating chemical reactions at the electrolyte/semiconductor interface and giving rise to larger current⁵⁵. Moreover, a temperature increase within a certain range can enhance the photoresponse of photodetectors⁵⁶.

In the revised Supplementary Information, we have added Figure R5: Supplementary Figure 17

Comment 9. Although the authors mentioned a dual-mode function of their device, ultimately, PSC and PSV cannot be used simultaneously as only one of them functions at a time. Along with this point, it would be better to mention the further challenges of their work.

[Response]

We appreciate your insightful comments on the device operation modes. Indeed, as pointed out by the reviewer, the photoelectrochemical synaptic device operates either in closed-circuit or open-circuit mode, limiting it to function in only one mode at a time. This is a common limitation for multi-modal devices, which typically can only operate in a single mode at a time [*Adv. Mater.* **35**, 2308090 (2023); *ACS Nano* **16**, 568–576 (2022)]. Additionally, due to the dual-modal characteristic, which differs from previous devices operating using a single signal, we need to design peripheral circuits capable of simultaneously reading both current and voltage signals. While the dual-modal feature offers switchable operational modes and synaptic behaviors, it also requires further research to meet the demands of multifunctional applications. In our future work, we aim to leverage the CMOS-compatible and low-cost silicon platform, along with micro/nano-fabrication techniques, to develop large-scale photoelectrochemical synaptic device arrays. Furthermore, by developing peripheral readout circuits, the simultaneous application of PSC and PSV functions on a single chip can be realized.

We have incorporated the above content into the Discussion section of revised manuscript:

In the photoelectrochemical synapse, while the dual-modal feature offers switchable operational modes and synaptic behaviors, it also requires further research to meet the demands of multifunctional applications. In our future work, we aim to leverage the CMOS-compatible and low-cost silicon platform, along with micro/nano-fabrication techniques, to develop large-scale photoelectrochemical synaptic device arrays. Furthermore, by developing peripheral readout circuits, the simultaneous application of PSC and PSV functions on a single chip can be realized.

Comment 10. As a minor comment, please clarify the positive and negative signs in the main figures and describe the direction of the electric field with arrows. Since multiple reactions occur simultaneously in this manuscript, the reviewer thinks the readers can be easily confused.

[Response]

We are grateful for your suggestions on improving the readability of our manuscript.

Regarding the polarity of electrical signals: our device operates in either current or voltage mode, with the electrical response signals exhibiting opposite polarities in each mode, as illustrated in **Figure R6a** and **b**. The relationship between the direction of charge carrier movement and the polarity of current (voltage) in our device is described as follows: (1) In current mode, when electrons flow towards the electrolyte, the current is negative; when electrons move towards the semiconductor and external circuit,

the current is positive. (2) In voltage mode, electron movement towards the electrolyte produces a positive voltage spike, while electron movement towards the semiconductor leads to a negative voltage spike. To enhance the readability of our manuscript, we have added following content on polarity definition in the revised manuscript: Additionally, for clarity, the relationship between the direction of charge carrier movement and the polarity of current (voltage) in our device is schematically shown in Supplementary Figure 9 and described as follows: In current mode, when electrons flow towards the electrolyte, the current is negative; when electrons transfer towards the external circuit, the current is positive. In voltage mode, electron movement towards the electrolyte produces a positive voltage spike, while electron movement towards the Si substrate leads to a negative voltage spike. The electrical signal polarity definitions are summarized in Supplementary Note 7.

We have added schematic and descriptions defining the polarities of electrical responses in the revised Supplementary Information: Supplementary Note 7. Current (voltage) signal polarity definition and electric field discussion

In Fig. 5 a, b, and c of the main text, we take the absolute value of the postsynaptic current (PSC) for performance comparison and have supplemented an explanatory note in the revised manuscript: Note that we take the absolute value of the postsynaptic current ($-\Delta PSC$) for performance comparison in Fig. 5a, b, and c.

Regarding the direction of the electric field: The electric fields in our device involve the electrolyte/p-AlGa_N and p-AlGa_N/n-GaN junctions, as shown in **Figure R6c**. Since we use arrows in the manuscript to indicate the direction of charge carrier transport, to avoid any confusion, we have supplemented descriptions and diagrams defining the direction of the electric field in the revised Supplementary Information: Supplementary Note 7. Current (voltage) signal polarity definition and electric field discussion

In the revised manuscript, we have added following content to illustrate the electric fields: We use arrows to depict the direction of the built-in electric fields, as shown in Supplementary Figure 9, indicating that the directions of the two electric fields are opposite.

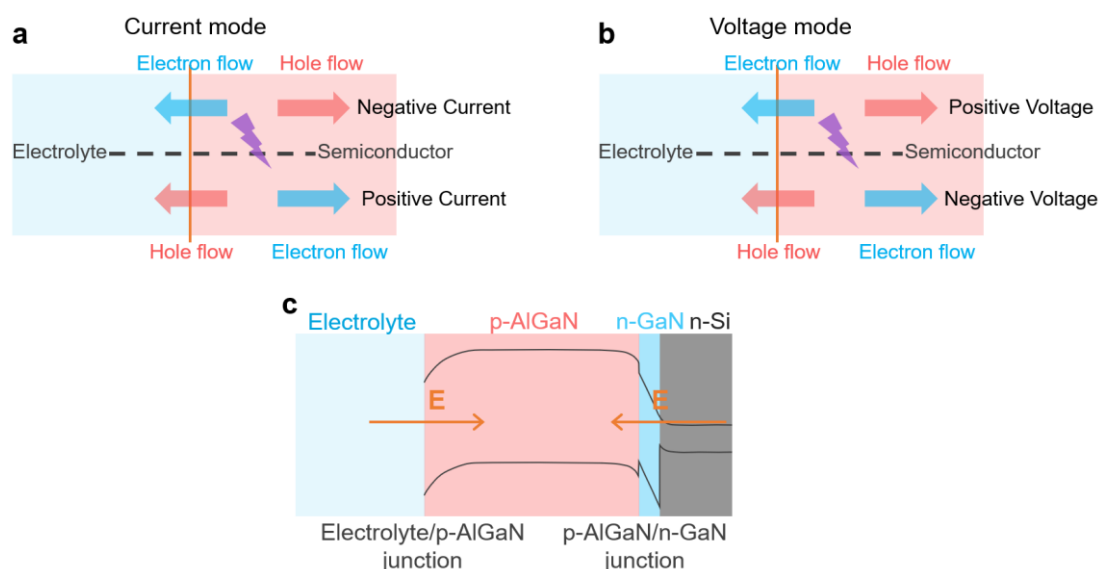


Figure R6. (a, b) Schematic illustrations of the polarity definitions for postsynaptic current (a) and postsynaptic voltage (b) in the photoelectrochemical synapse. (c) Schematic of the built-in electric fields, indicating the opposite directions of the two fields.

Reviewer #2:

Overall comment: Liu et al. demonstrates a novel photoelectrochemical synaptic device based on p-AlGaIn/n-GaN nanowires. By applying such synaptic device in close- or open-circuit, it can exhibit either short-term or long-term plasticity behavior. While the manuscript is novel and of interest to the community, the following questions should be addressed before it may be granted for publication at Nature Communications.

[Overall response]

We appreciate your review and insightful comments, which are crucial for enhancing the quality and readability of our manuscript.

Comment 1. Authors come up with an explanation of the short-term plasticity when the device is applied in close circuit. Extra carriers stimulated by the short laser pulse will flow to both the Pt electrode and end of p-AlGaIn to incorporate in the redox reaction with aqueous electrolyte. As what depicted in Fig. 3d, electrolysis of water is considered as the redox reaction happened in the electrolyte. However, authors don't provide experimental evidence of generating hydrogen and oxygen when redox reaction happens.

[Response]

Thank you for the valuable comments regarding the interface redox reactions. To clarify this, we have supplemented mechanism analysis and experimental evidence. The detailed discussions are as follows:

A. Mechanism analysis of redox reaction: As shown in **Figure R7**, the conduction and valence band edges of AlGaIn straddle water redox potentials. When p-AlGaIn is immersed in an aqueous electrolyte and exposed to light above the bandgap, the photogenerated electrons and holes separate, transport, are then consumed by the aqueous electrolyte. These electrons flow into the electrolyte to undergo hydrogen generation reactions ($4e^- + 4H^+ \rightarrow 2H_2$), while holes flow to the Pt electrode to undergo oxygen generation reactions ($4h^+ + 2H_2O \rightarrow O_2 + 4H^+$). Such phenomenon has been widely demonstrated and discussed in previous researches [*Nat. Commun.* **6**, 6797 (2015); *Nature* **613**, 66–70 (2023)]. Additionally, GaN-based materials including InGaIn, GaN, and AlGaIn have been widely used for hydrogen and oxygen generation via water splitting [*Nat. Commun.* **6**, 6797 (2015); *Nature* **613**, 66–70 (2023)].

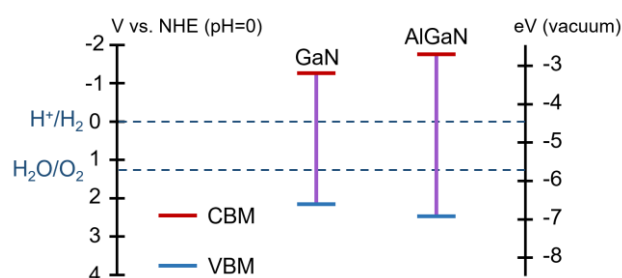


Figure R7. Schematic diagram of the GaN and AlGaIn band structures.

B. Experimental evidence of redox reaction: In our device, when p-AlGaIn is illuminated by photons with energy greater than the bandgap, photo-electric process occurs, generating charge carriers. These charge carriers separate, transport, and ultimately undergo redox reactions with the aqueous electrolyte, being consumed via water splitting to produce hydrogen and oxygen. However, in our tests, due to the small current of nA level and short duration of 10^2 s, the gas produced is at the order of 10^{-10} L. Considering the solubility of H_2 in water, which is approximately 1.83 ml H_2 /100 ml, it is difficult to

directly detect the generated hydrogen and oxygen in our regular tests. To further demonstrate the generation of hydrogen and oxygen, we increased the applied voltage and duration (i.e., extreme condition) to accumulate gas output. After both regular and extreme tests, we used inert argon (Ar) to purge the gases from the sealed chambers and collected them in gas bags. Then, we analyzed the collected gases using gas chromatograph (Agilent 8860 gas chromatograph). Before the gas chromatography tests, we cleaned the chromatograph instrument with Ar. It should be noted that during the gas detection process, we collect the produced gases using gas bags and then inject the gases into the chromatograph for analysis, which is offline test. Inevitably, trace amounts of air might be introduced, including at the chromatograph's inlet. **Figure R8a** shows the result after the regular test (0 V, 100 s), revealing signal peaks for O₂ and N₂, but none for H₂. The absence of an H₂ signal is due to the extremely low gas production, while the observed O₂ and N₂ signals are mainly because trace amounts of air were introduced during the offline test process. To better illustrate the redox reactions occurring in the device (i.e., H₂ generation at the nanowire electrode and O₂ generation at the Pt electrode), we utilized an H-shaped cell for analysis. The nanowire electrode and Pt electrode were placed in two separate chambers, connected by a proton exchange membrane (Nafion 117 film). This type of cell is widely used in studies of hydrogen and oxygen production [*Chem. Eng. Sci.* **104**, 125–146 (2013); *Adv. Energy Mater.* **12**, 2201358 (2022)]. After the extreme test (-0.5 V, 1 h), we collected gases from each chamber using gas bags and performed gas chromatography analysis. For the nanowire electrode, a significant H₂ peak was observed, confirming the production of H₂ (**Figure R8b**). Additionally, minor peaks for O₂ and N₂ were observed, which are consistent with the result under regular conditions and are attributed to the offline test process. For the Pt electrode, a significant O₂ peak was detected, with the intensity of the O₂ peak being much greater than that of the N₂ peak (**Figure R8c**). Compared to the result in **Figure R8a**, the O₂/N₂ intensity ratio is significantly different, which rules out the interference from the offline test process and confirms the production of O₂.

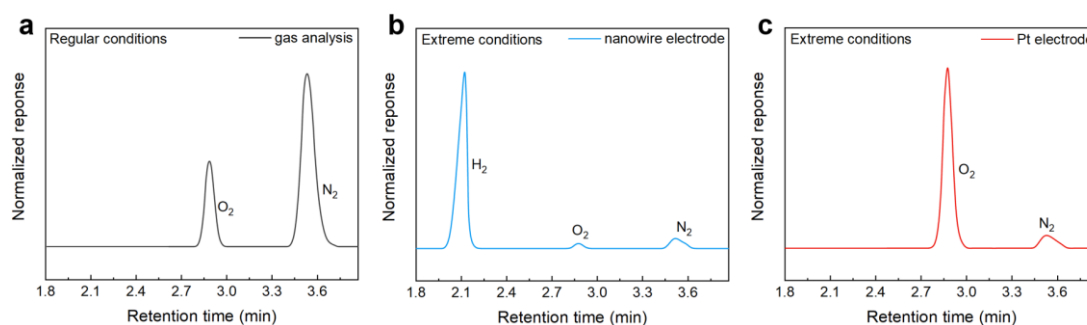


Figure R8. Gas chromatography analysis. (a) Results under regular conditions (0 V, 100 s). (b, c) Results under extreme conditions (-0.5 V, 1 h).

In the revised manuscript, we have supplemented the following content to provide a detailed explanation of the interface redox reactions: When electrons are consumed by the aqueous electrolyte ($4e^- + 4H^+ \rightarrow 2H_2$), corresponding holes flow to Pt electrode and are consumed by the electrolyte ($4h^+ + 2H_2O \rightarrow O_2 + 4H^+$), due to the conduction and valence band edges of AlGaN straddle water redox potentials^{33,42}. Additionally, we conducted gas chromatography analysis to verify the generation of H₂ and O₂ under extreme test conditions (i.e., high applied bias, long duration), as shown in Supplementary Figure 11. Detailed discussion on interface redox reactions can be found in Supplementary Note 8.

In the revised Supplementary Information, we have included above discussions on redox reaction and Figure R8: Supplementary Note 8. Detailed processes of the chemical-electric behavior

Comment 2. Authors showcase the concentration of H₂SO₄ in electrolyte can modulate the short-term response of the device, while Na₂SO₄ doesn't significantly affect device's performance. It indicates that proton plays an important role in the redox reaction. Similar to my first question, since authors don't provide evidence of generating hydrogen, it is possible that proton react with the p-AlGa_{0.5}N. More characterization should be implemented to figure out the details of the redox reaction.

[Response]

Thank you for your valuable insights into the working mechanism of our device. In response to the first comment, we have supplemented gas chromatography analysis to demonstrate that the redox reactions at the interface involve water splitting. Indeed, as you mentioned, protons play a crucial role in redox reactions. In the hydrogen evolution reaction between protons and electrons ($2e^- + 2H^+ \rightarrow H_2$), the concentration of protons significantly affects the reaction rate. As the proton concentration increases, the reaction between electrons and protons accelerates, resulting in an increase in the negative current response [*Light: Sci. Appl.* **11**, 227 (2022); *Nat. Commun.* **11**, 5179 (2020)]. Therefore, in our device, by altering the H₂SO₄ concentration or pH value to change the proton concentration, we can effectively modulate the synaptic response. In contrast, increasing the Na₂SO₄ concentration increases the concentration of conductive ions, leading to the facilitated consumption of both electrons and holes. In this context, the holes flowing to the external circuit decrease, resulting in a decrease in the negative current. When water is replaced with Na₂SO₄ solution, the postsynaptic current decreases. However, further increasing the sodium sulfate concentration exhibits little effect, possibly because the influence of electrolyte conductivity has already reached saturation.

Additionally, GaN-based nanowires grown by MBE, including InGa_{0.5}N, GaN, and AlGa_{0.5}N, have been extensively utilized for hydrogen and oxygen production in acidic environments, exhibiting excellent long-term stability [*Nat. Commun.* **14**, 2047 (2023); *Nat. Commun.* **14**, 179 (2023)]. GaN-based materials are highly stable in acidic environments and do not react with protons [*Nano Lett.* **13**, 4356–4361 (2013); *Analyst* **143**, 2784–2789 (2018)].

In the revised Supplementary Information, we have included the above discussions in [Supplementary Note 8. Detailed processes of the chemical-electric behavior](#)

Comment 3. As authors predicted, coating of Pt nanoparticles on device can facilitate the reaction through the interface of electrolyte/p-AlGa_{0.5}N. The negative portion of the PSC when laser pulse is on is obviously enhanced with Pt coating as authors' prediction, however, for the first pulse in Fig. 4e, why can we still get some positive PSC during 10.0 s to ~10.02 s if the reaction happens at the interface is much faster than going through the circuit.

[Response]

We appreciate your insightful comments. In fact, compared to the carrier drift within the p-n junction and circuit, the chemical reaction and carrier consumption at the interface are slower. Even though loading Pt accelerates the chemical reaction at the interface, it is still slower than the carrier transport within the semiconductor [*ACS Nano* **12**, 11088 (2018)]. This inevitably leads to a small number of electrons flowing to the external circuit through the p-n junction, manifested as the small positive PSC peak observed at the initial stage.

Redox reactions at the semiconductor/electrolyte interface occur within the time scale of $\sim 10^{-3}$ s [*ACS Nano* **12**, 11088 (2018)], whereas semiconductor internal carrier transport occurs in the time range of $\sim 10^{-9}$ s [*ACS Nano* **12**, 11088 (2018)]. Note that these time constants are provided for reference only.

Considering our device operates in aqueous environment, the photo-electric and chemical-electric processes are closely connected, making it challenging to measure the specific time required for above two processes. In future work, we will attempt to conduct in-situ time-resolved analyses to study the time-resolved charge carrier dynamics of the distinctive synaptic behaviors. Therefore, although Pt modification significantly accelerates the transport and consumption of interface carriers, as evidenced by the reduction in positive PSC peak and boosted negative PSC response after Pt loading, the required time for interface chemical reactions still exceeds that of semiconductor internal carrier transport [*ACS Nano* **12**, 11088 (2018)]. This results in a small number of electrons flowing to the external circuit through the p-n junction, manifested as the small positive PSC peak.

In the revise manuscript, we have added the following content to explain the small positive PSC peak at initial stage: Notably, a small positive PSC peak can be observed at the initial stage (inset of Fig. 4e), which is attributed to the fact that, even though Pt nanoparticle decoration accelerates the interface chemical reactions, the chemical reactions and carrier consumption at the interface are still slower than the carrier drift within the semiconductor and circuit⁴³. This inevitably leads to a small number of electrons flowing to the external circuit, manifested as the observed small positive PSC spike (detailed discussion is provided in Supplementary Note 5).

In the revised Supplementary Information, we have added the detailed discussion: Supplementary Note 5. The quantitative comparison of the photo-electric and chemical-electric processes

Comment 4. Concentration of H₂O₂ is a signal of aging and decline of human's cognitive. However, authors should provide more explanation on why H₂O₂ can suppress device's synaptic behavior. As what I mentioned in my first two questions, authors provide limited explanation on the redox reaction happening between the electrolyte and p-AlGaIn, so that although authors provide many methods of modifying the electrolyte such as adding proton, AA, or H₂O₂ to control device's synaptic behavior, the mechanism still confuses me.

[Response]

Thank you for your valuable suggestions on the device working mechanism. We apologize for not discussing in detail the mechanisms of the redox reactions and how chemical changes affect synaptic responses. In response to your first two comments, we have supplemented detailed theoretical analysis and experimental evidence of redox reactions. Altering the chemical environment of the electrolyte affects the redox reactions between electrons/holes and the electrolyte, thereby influencing the transport of electrons/holes to the external circuit and ultimately regulating device synaptic responses, as schematically illustrated in **Figure R9a**. In our study, we focused on altering proton concentration (i.e., H₂SO₄ concentration and pH value), varying the concentration of conductive ions (Na₂SO₄ concentration), adding ascorbic acid, and adding H₂O₂. The detailed regulation mechanisms are as follows:

0) Default Condition: When the chemical environment of the electrolyte remains unchanged, electrons and holes are consumed through the redox reactions of water splitting. In our device, the semiconductor electrode determines the polarity and magnitude of the photoresponse. Therefore, we discuss the consumption of electrons and holes at the semiconductor/electrolyte interface. At the semiconductor/electrolyte interface, under default conditions, the primary chemical reaction involve electron consumption reaction ($4e^- + 4H^+ \rightarrow 2H_2$). This corresponds to holes flowing towards the circuit, which are recorded by the instrument as negative current. Moreover, a faster electron consumption rate (i.e., more holes flowing to the circuit) corresponds to a larger negative current.

1) Proton Concentration: In the reaction between protons and electrons ($2e^- + 2H^+ \rightarrow H_2$), the concentration of protons significantly influences the reaction rate. As the proton concentration increases, the reaction between electrons and protons accelerates, leading to an increase in the negative current response [*Light: Sci. Appl.* **11**, 227 (2022); *Nat. Commun.* **11**, 5179 (2020)]. Therefore, in our device, by adjusting the H_2SO_4 concentration and pH value to alter the proton concentration, the synaptic response of the device can be significantly regulated. As the H_2SO_4 concentration increases and the pH value decreases, the synaptic response of the device increases notably (**Figure R9b**).

2) Conductive ions concentration: Increasing the concentration of conductive ions is equivalent to increasing the conductivity of electrolyte. The consumption rates of electrons and holes at the semiconductor/electrolyte interface both increase. In this context, the holes flowing to the external circuit decrease, resulting in a decrease in the negative current (**Figure R9b**). Therefore, when water is replaced with Na_2SO_4 solution, the postsynaptic current decreases, which is consistent with previous report [*Light: Sci. Appl.* **11**, 227 (2022)]. However, further increasing the Na_2SO_4 concentration has little effect. This may be explained by considering that the increased conductivity of the electrolyte solution no longer significantly impacts the synaptic performance, indicating that the influence of electrolyte conductivity has reached saturation.

3) Adding ascorbic acid (AA): AA, which is a common electron donor, can undergo oxidation reactions with holes ($AA + h^+ \rightarrow$ dehydro-ascorbic acid). This hole consumption reaction can easily happen, which is more favorable than the default hole consumption reaction [*Nano Energy* **34**, 392–398 (2017); *Electrochim. Acta* **404**, 139746 (2022)]. Therefore, AA can capture holes and facilitates hole consumption at the semiconductor/electrolyte interface. As a result, the holes flowing to the external circuit decrease, leading to a decrease in synaptic responses (**Figure R9b**).

4) Adding H_2O_2 : H_2O_2 is widely used as hole scavenger ($H_2O_2 + 2h^+ \rightarrow O_2 + 2H^+$). This hole consumption reaction can easily happen, which is more favorable than the default hole consumption reaction [*ACS Energy Lett.* **3**, 307–314 (2018); *ACS Appl. Mater. Interfaces* **8**, 34490–34496 (2016)]. In our device, H_2O_2 can capture holes and promotes hole consumption at the electrolyte/semiconductor interface and reduces the holes flowing to the external circuit, resulting in a decrease in the synaptic response (**Figure R9b**). Note that although protons are generated when H_2O_2 is consumed, the electrolyte used is PBS buffer solution, and the pH of the solution remains constant (i.e., the proton concentration remains unchanged).

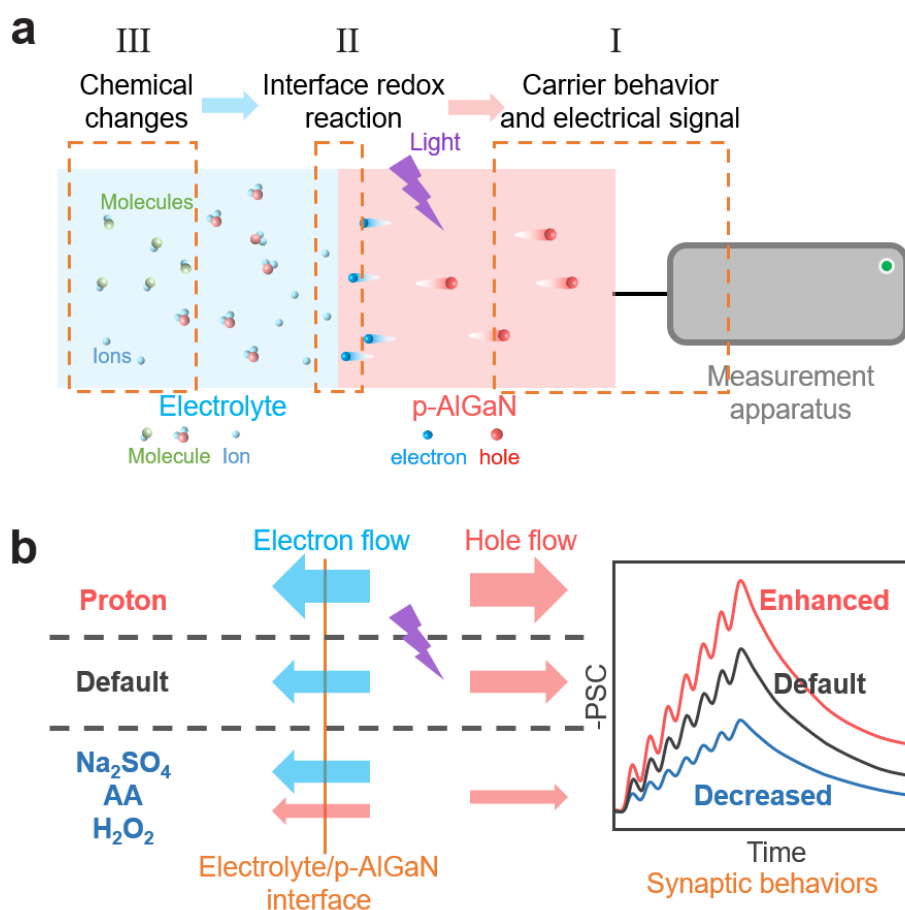


Figure R9. (a) Schematic diagram illustrating the chemical-electric process at the p-AlGaN/electrolyte interface. (b) Schematic illustrating the impact of changing chemical environments on synaptic responses. "Default" refers to the default electrolyte environment without changing the chemical surroundings.

In the revised manuscript, we have modified and added the modulation mechanisms of changing H₂SO₄ and Na₂SO₄ concentrations, changing pH value, adding AA, and introducing H₂O₂:

The regulation mechanism of H₂SO₄ solution is primarily attributed to change in proton concentration: the chemical reaction on p-AlGaN nanowires mainly involves the reduction reaction between protons and electrons ($2e^- + 2H^+ \rightarrow H_2$), in which the proton concentration significantly affects the reaction rate. As the proton concentration increases, the chemical reaction between electrons and protons accelerates, leading to the boosted negative current response^{36,52}. Thus, increasing the H₂SO₄ concentration significantly enhance the synaptic response. When water is replaced with Na₂SO₄ solution, the concentration of conductive ions (i.e., conductivity of the electrolyte) increases, leading to an increased consumption rate of both electrons and holes at the semiconductor/electrolyte interface. In this context, fewer holes flow to the circuit, resulting in a reduced negative current, manifested as the diminished postsynaptic current, consistent with previous report³⁶. Further increasing the Na₂SO₄ concentration has little effect, which may be explained by considering that the increased conductivity of the electrolyte solution no longer significantly impacts synaptic performance, indicating that the influence of electrolyte conductivity has reached saturation. Additionally, the pH-dependent synaptic response was explored, as shown in Fig. 5b. As the pH value decreases, the postsynaptic current is noticeably enhanced due to the increased proton concentration. More detailed discussion on mechanisms of chemical regulation effect is provided in Supplementary Note 8.

The molecule regulation effect arises from the electron donor role of AA, which can undergo oxidation reactions with holes ($AA + h^+ \rightarrow$ dehydro-ascorbic acid). This hole consumption reaction can easily happen and is more favorable than the default hole consumption reaction in aqueous electrolyte^{53,54}. AA can capture holes and considerably facilitates hole consumption at the semiconductor/electrolyte interface. As a result, the holes flowing to the external circuit decrease, leading to the decrease in postsynaptic current.

The diminished synaptic responses are due to the hole scavenger role of H_2O_2 ($H_2O_2 + 2h^+ \rightarrow O_2 + 2H^+$), which can easily happen and is more favorable than the default hole consumption reaction in aqueous electrolyte⁵⁹. H_2O_2 can capture holes and facilitates hole consumption at the electrolyte/semiconductor interface and reduces the holes flowing to the external circuit, resulting in the weakened synaptic behaviors. It is noteworthy that although protons are generated when H_2O_2 is consumed, the electrolyte used is PBS buffer solution, and the pH remains essentially unchanged. More detailed discussion of the H_2O_2 regulation effect is provided in Supplementary Note 8.

In the revised Supplementary Information, we have added detailed chemical modulation mechanisms and schematic illustrations in Supplementary Note 8. Detailed processes of the chemical-electric behavior

Reviewer #3:

Overall comment: The authors reported a photoelectrochemical synaptic device based on p-AlGaIn/n-GaN semiconductor nanowires for emulating the chemical-electric synaptic processes. STP and LTP of the device were modulated by switching the closed and open circuits, respectively. The synaptic responses were amplified with the use of Pt nanoparticles onto nanowire surfaces. The optoelectronic synapses were presented to show the modulation by employing the chemical-electric manner. However, before considering its publication, some critical issues need to be addressed.

[Overall response]

We sincerely appreciate your review and suggestions to improve the quality of our manuscript.

Comment 1. Many types of material systems, including transition oxide, and van der Waals 2D materials, are developed to electronic or optoelectronic synapses. Why did you use the materials of GaN-based systems? Please give a more detailed explanation.

[Response]

We are grateful for your insightful comments. In our work, we employ p-AlGaIn/n-GaN nanowires due to their exceptional optoelectronic characteristics and chemical properties, as well as their promising scalability for future development. The detailed rationale is outlined below:

(1) Excellent optoelectronic characteristics: GaN is a direct bandgap semiconductor material, making it suitable for fabricating optoelectronic devices. When they are grown by plasma-assisted molecular beam epitaxy (MBE), GaN nanowires exhibit high crystallinity and large surface-to-volume ratio, giving rise to superior light absorption and charge carrier behaviors, rendering them as great material candidates in building optoelectronic devices [*Nat. Electron.* **4**, 645–652 (2021); *Adv. Mater.* **36**, 2307779 (2024)].

(2) Superior material for chemical-related applications: GaN material demonstrates chemical stability in aqueous solutions, thereby widely applied in studies involving electrolyte-mediated chemical reactions [*Nature* **613**, 66–70 (2023)]. Furthermore, the one-dimensional structure of nanowires provides a large surface area, making them highly sensitive to electrolyte solutions and thus ideal for constructing synaptic devices with chemical-related functionalities. The photoelectrochemical synapse leverages the interplay of photo-electric and chemical-electric processes to achieve various synaptic functions. GaN materials exhibit excellent performance in optoelectronic and chemical-related device applications, making them an ideal choice for our photoelectrochemical synapse.

(3) Controllable material growth and promising scalability: The growth of GaN material is highly controllable with the epitaxy techniques such as MBE or metal organic chemical vapor deposition (MOCVD) enabling precise control over alloy composition (e.g., AlGaIn or InGaIn) and doping concentration. This controllable growth processes enhances the scalability of GaN materials. By regulating the alloy composition in GaN, the bandgap can be tuned, allowing the material system to cover a broad spectrum ranging from the ultraviolet to the near-infrared [*Nat. Mater.* **6**, 951–956 (2007)]. This capability facilitates future research on optoelectronic synapses with a broad spectral response.

(4) Potential integration with other device: Notably, GaN-based systems have been widely used in developing optoelectronic devices (e.g., photodetector, LED), electronic devices (e.g., high-electron-mobility transistor, Schottky barrier diode), and piezoelectric pressure sensors. Through rational device structure design and advanced micro-nano fabrication processes, our device could be integrated with these devices. Additionally, the GaN nanowires used in our device are based on a CMOS-compatible and low-cost silicon platform, highlighting its great promise in future integrated Si-photonics applications.

In the revised manuscript, we have included the clarification of the advantages of GaN-based nanowires: GaN materials exhibit excellent optoelectronic and piezoelectric properties^{21,26}. In recent years, there have been notable works utilizing GaN materials, including micro/nanowires and cantilever structures, for the development of strain-sensitive electrical synapses²⁶⁻³⁰ and optoelectronic synapses^{31,32}. GaN materials demonstrate good chemical stability in electrolyte solution, making it suitable for researches involving electrolyte-mediated chemical reactions³³. Furthermore, GaN materials exhibit tunable bandgap and show promising prospects for device integration³⁴. During epitaxial growth, the bandgap of GaN materials can be controlled by adjusting the alloy composition (e.g., AlGa_N or InGa_N), enabling the material system to cover a broad spectrum from ultraviolet to near-infrared³⁴. More importantly, GaN-based nanowires, characterized by outstanding crystallinity and large surface-to-volume ratio, are particularly attractive in optoelectronic applications due to their superior light absorption and charge carrier behaviors^{33,35}. Additionally, in an aqueous environment, the large surface area of the one-dimensional structure makes the nanowires exceptionally sensitive to electrolyte solutions^{36,37}, ideal for constructing optoelectronic synapses with chemical-related functions.

Comment 2. In recent years, some timely and significant works presented nitride-based materials, such as micro/nanowire, and cantilever-structured GaN, for developing novel memristors or synapses. However, this paper does not cite any reference to the field. Please add such related citations.

[Response]

Thank you for the valuable comments. In recent years, there have been several outstanding reports on synaptic devices and memristors based on GaN materials. These works not only leverage the excellent photo-electric effect of GaN to construct optoelectronic synapses but also utilize the unique piezoelectric effect to develop strain-sensitive electrical synapses.

To provide readers with a comprehensive understanding of GaN-based synaptic devices, we have incorporated the following content into the revised manuscript: GaN materials exhibit excellent optoelectronic and piezoelectric properties^{21,26}. In recent years, there have been notable works utilizing GaN materials, including micro/nanowires and cantilever structures, for the development of strain-sensitive electrical synapses²⁶⁻³⁰ and optoelectronic synapses^{31,32}.

In References, we have added:

26. Zhang, S. et al. Strain-controlled power devices as inspired by human reflex. *Nat. Commun.* **11**, 326 (2020).

27. Hua, Q. et al. Piezotronic Synapse Based on a Single GaN Microwire for Artificial Sensory Systems. *Nano Lett.* **20**, 3761–3768 (2020).

28. Zhou, X. et al. Magnetosensory Power Devices Based on AlGa_N/Ga_N Heterojunctions for Interactive Electronics. *Adv. Electron. Mater.* **9**, 2200941 (2023).

29. Hua, Q. et al. Flexible GaN microwire-based piezotronic sensory memory device. *Nano Energy* **78**, 105312 (2020).

30. Liu, H. et al. A Bamboo-Like GaN Microwire-Based Piezotronic Memristor. *Adv. Funct. Mater.* **26**, 5307–5314 (2016).

31. Hong, X. et al. Two-Dimensional Perovskite-Gated AlGa_N/Ga_N High-Electron-Mobility-Transistor for Neuromorphic Vision Sensor. *Adv. Sci.* **9**, 2202019 (2022).

32. Chang, K.-C. et al. Optoelectronic Dual-Synapse based on Wafer-level GaN-on-Si Device Incorporating Embedded SiO₂ Barrier Layers. *Nano Energy* **125**, 109564 (2024).

Comment 3. Synapse is a kind of ultralow power device for emerging computing architecture. The device shows a reasonably large leakage current level of nA. Could you comment on that?

[Response]

Thank you for the instructive and valuable comment. In our device, upon removal of light stimulation, the current decays to its original state at the nA level. In recent years, numerous optoelectronic synapses with similar current scales (i.e., nA) have been reported, utilized for synaptic functions, artificial neuromorphic vision systems, and image recognition applications [*Adv. Mater.* **35**, 2308090 (2023); *Nat. Commun.* **14**, 7179 (2023); *Adv. Mater.* **36**, 2311524 (2024)]. Therefore, we believe that our device holds promise for building neuromorphic vision sensors for image sensing and memorization applications. In our future work, we aim to integrate micro/nano-fabrication techniques to further downscale the device dimensions (e.g. using only a cluster of nanowires in tens or hundreds), thereby decreasing the device current and power consumption for large-scale integration and applications. Additionally, compared with the nA level current observed in current mode, devices operating in voltage mode exhibit no static current and can work without an electric power supply, making it suitable for energy-efficient neuromorphic applications.

In the revised manuscript, we have added the following description: As displayed in Fig. 2, the photoelectrochemical synapse demonstrates current in the nA level in current mode. In future work, we aim to integrate micro/nanofabrication processes to further downscale the device dimensions, thereby lowering device current and power consumption.

Comment 4. High-resolution TEM characterization should be provided to represent the crystal structure of AlGa_{0.2}N/GaN.

[Response]

Thank you for the helpful suggestions. We conducted high-resolution TEM characterization of AlGa_{0.2}N/GaN, and the result is illustrated in **Figure R10**. The image reveals clear lattice fringes of the GaN materials, indicating the excellent crystallinity of nanowires grown through MBE.

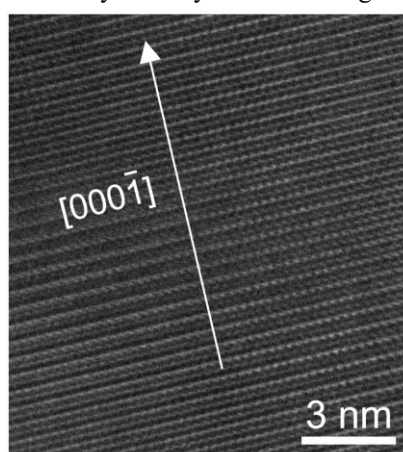


Figure R10. High-resolution TEM image, showing excellent crystallinity of MBE-grown nanowire.

In the revised manuscript, we have included description of the crystal structure: Additionally, we conducted high-resolution transmission electron microscopy (TEM) characterization of the as-prepared nanowires (Supplementary Figure 13), which reveals clear lattice fringes of the GaN materials, indicating the excellent crystallinity of the nanowires grown through MBE.

In the revised Supplementary Information, we have included the above-mentioned high-resolution

Comment 5. Please provide some experimental evidence to illustrate the interplay of optoelectronic and chemical-electric behavior for the GaN-based synapse. And the working mechanism should be talked more about.

[Response]

Thank you for the comments on the working mechanisms.

Interplay of photo-electric and chemical-electric behaviors: The photoelectrochemical synaptic device operates in an electrolyte environment. Under illumination and in current mode, photogenerated carriers are produced, and due to the two back-to-back built-in electric fields, holes are stored within the nanowires while electrons flow into the electrolyte to undergo chemical redox reactions (**Figure R11a**). In voltage mode, photogenerated carriers are also produced under illumination, and the downward band bending at the electrolyte/semiconductor interface drives electrons into the electrolyte, where they are consumed by positively charged species (**Figure R11a**). Overall, both operational modes leverage the interplay of photo-electric behaviors within the semiconductor and chemical-electric behaviors at the electrolyte/semiconductor interface for synaptic responses.

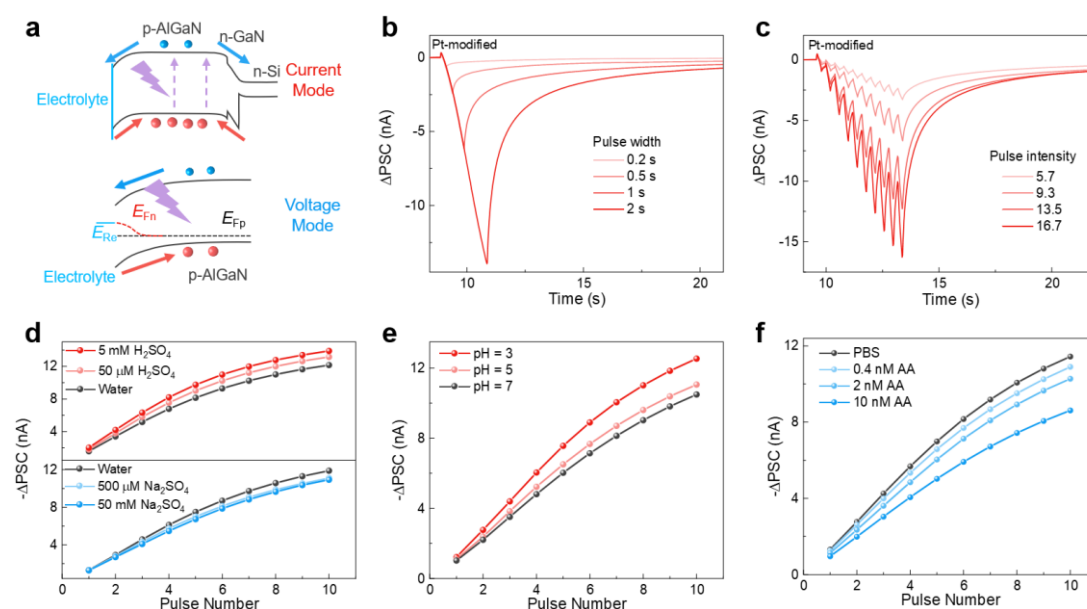


Figure R11. (a) Schematic of band bending and charge carrier behaviors under illumination in current mode (top) and voltage mode (bottom). The red and blue spheres represent photogenerated holes and electrons, respectively. (b, c) Postsynaptic current responses of Pt-modified synaptic device under different pulse durations (b) and pulse intensities (c). (d-f) Postsynaptic current responses of Pt-modified synaptic device in electrolyte environment with varying concentrations (d), different pH values (e), and different ascorbic acid concentrations (f).

By altering illumination conditions such as pulse duration and intensity, the photo-electric processes can be regulated, thereby modulating the synaptic responses (**Figure R11b** and **c**). Additionally, the chemical-electric processes can be tuned by varying chemical surroundings, such as changing the electrolyte concentration, adjusting pH value, and adding ascorbic acid, thus modulating the synaptic responses (**Figure R11d-f**). These experimental evidences demonstrate that both illumination and chemical conditions can affect the synaptic behaviors, highlighting the interplay of photo-electric and

chemical-electric processes, which collectively govern the synaptic responses. Furthermore, we fabricated a solid-state photodetector using p-AlGaIn/n-GaN nanowires, which only involves photo-electric processes, employing Ni/Au and Ti/Au for ohmic contacts. The device exhibited a typical photodetector response due to the p-n junction structure (**Figure R12**). This experimental evidence underscores the necessity of chemical-electric processes and the electrolyte environment in constructing a photoelectrochemical synapse. In summary, above band structure analysis and experimental evidences elucidate the interplay of photo-electric and chemical-electric processes, collectively determining the synaptic responses.

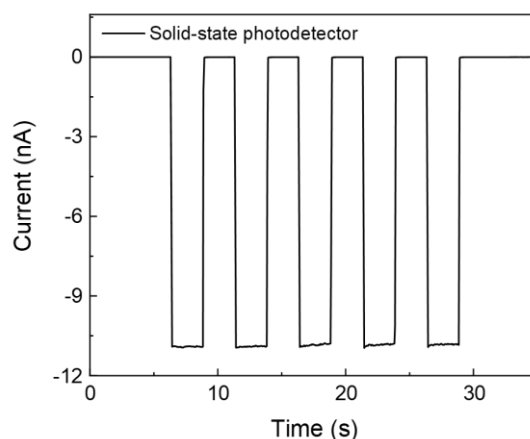


Figure R12. Photocurrent response of solid-state device based on p-AlGaIn/n-GaN nanowires.

Regarding the working mechanisms, we have elaborated below in details on how chemical alterations regulate synaptic behavior. In our study, we focused on altering proton concentration (i.e., H_2SO_4 concentration and pH value), varying the concentration of conductive ions (Na_2SO_4 concentration), adding ascorbic acid, and adding H_2O_2 . Altering the chemical environment of the electrolyte affects the redox reactions between electrons/holes and the electrolyte, thereby influencing the transport of electrons/holes to the external circuit and ultimately regulating device synaptic responses. The detailed analyses are as follows:

0) Default Condition: When the chemical environment of the electrolyte remains unchanged, electrons and holes are consumed through the redox reactions with electrolyte. In our device, the semiconductor electrode determines the polarity and magnitude of the photoresponse. Therefore, we discuss the consumption of electrons and holes at the semiconductor/electrolyte interface. At the semiconductor/electrolyte interface, under default conditions, the primary chemical reaction involve electron consumption through proton reduction. This corresponds to holes flowing towards the circuit, which are recorded by the instrument as negative current. Moreover, a faster electron consumption rate (i.e., more holes flowing to the circuit) corresponds to a larger negative current.

1) Proton Concentration: In the chemical reaction between protons and electrons, the concentration of protons significantly influences the reaction rate. As the proton concentration increases, the reaction between electrons and protons accelerates, leading to an increase in the negative current response [*Light: Sci. Appl.* **11**, 227 (2022); *Nat. Commun.* **11**, 5179 (2020)]. Therefore, in our device, by adjusting the H_2SO_4 concentration and pH value to alter the proton concentration, the synaptic response of the device can be significantly regulated. As the H_2SO_4 concentration increases and the pH value decreases, the synaptic response of the device increases notably.

2) Conductive ions concentration: Increasing the concentration of conductive ions is equivalent to

increasing the conductivity of electrolyte. The consumption rates of electrons and holes at the semiconductor/electrolyte interface both increase. In this context, the holes flowing to the external circuit decrease, resulting in a decrease in the negative current. Therefore, when water is replaced with Na₂SO₄ solution, the postsynaptic current decreases, which is consistent with previous report [*Light: Sci. Appl.* **11**, 227 (2022)]. However, further increasing the Na₂SO₄ concentration has little effect. This may be explained by considering that the increased conductivity of the electrolyte solution no longer significantly impacts the synaptic performance, indicating that the influence of electrolyte conductivity has reached saturation.

3) Adding ascorbic acid (AA): AA, which is a common electron donor, can undergo oxidation reactions with holes. This hole consumption reaction can easily happen [*Nano Energy* **34**, 392–398 (2017); *Electrochim. Acta* **404**, 139746 (2022)]. Therefore, AA can capture holes and facilitates hole consumption at the semiconductor/electrolyte interface. As a result, the holes flowing to the external circuit decrease, leading to a decrease in synaptic responses.

4) Adding H₂O₂: H₂O₂ is widely used as hole scavenger and can undergo oxidation reactions with holes. This hole consumption reaction can easily happen [*ACS Energy Lett.* **3**, 307–314 (2018); *ACS Appl. Mater. Interfaces* **8**, 34490–34496 (2016)]. In our device, H₂O₂ can capture holes and promotes hole consumption at the electrolyte/semiconductor interface and reduces the holes flowing to the external circuit, resulting in a decrease in the synaptic response.

The above band structure analysis and experimental tests can be found in the original manuscript. In the revised manuscript, we have additionally included the following discussion on the necessity of chemical-electric processes (i.e., experimental test of the solid-state device):

To further illustrate the necessity of the electrolyte/semiconductor junction, we fabricated solid-state devices using p-AlGaIn/n-GaN nanowires and tested the photoresponse, as shown in Supplementary Figure 5. The solid-state device exhibits typical photodetector behaviors due to the p-n junction. In the photoelectrochemical synapse, the electrolyte environment creates a downward surface band bending at the p-AlGaIn/electrolyte interface, thereby introducing two opposite built-in electric fields for carrier storage and synaptic behavior.

In the revised Supplementary Information, we have added the discussion on solid-state photodetector in Supplementary Note 4, and the detailed chemical regulation mechanisms in Supplementary Note 8:

Supplementary Note 4. Working mechanism validation based on other nanowire samples and device structure

Supplementary Note 8. Detailed processes of the chemical-electric behavior

Comment 6. The author tested the devices using an electrochemical workstation, and there may be curve drift during testing. Will there be any changes in the performance of the devices?

[Response]

Thank you for the valuable comments on experimental testing. In our device, we extended the measurement time for both current and voltage modes, as depicted in **Figure R13**. Throughout the device testing, we did not observe significant curve fluctuations or drift affecting the device performance. Electrochemical workstations have been widely utilized for long-term performance evaluation, including studies on photoelectrochemical photodetectors [*ACS Appl. Mater. Interfaces* **14**, 7175–7183 (2022); *Adv. Electron. Mater.* **5**, 1900726 (2019)], with no reported instances of curve drift affecting device performance. Moreover, there are reports of using source meters for photoelectrochemical device testing [*ACS Nano* **18**, 652–661 (2024)]. In future experiments, we can consider changing the measurement

instruments or conducting pre-calibration of the measurement apparatus to avoid potential curve drift and its impact on device performance.

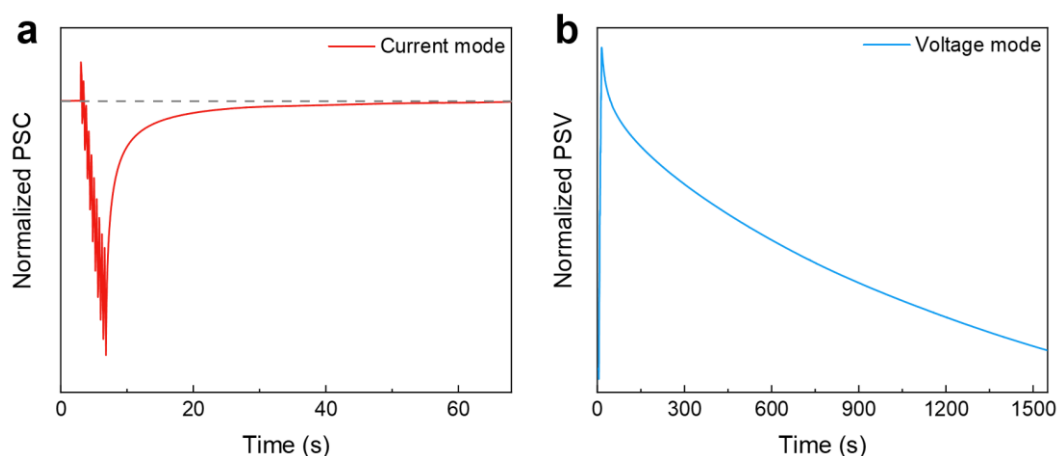


Figure R13. Device performance in current mode (a) and voltage mode (b) with extended measurement time.

Comment 7. The photoelectrochemical synapse operated in current mode (STP) or voltage mode (LTP) by altering the circuit state (either closed-circuit or open-circuit). It is confused for synaptic updates when compared to the reported synapses. Could you explain why uses such operations of circuit state?

[Response]

Thanks for your insightful comments on the device operation modes. In our work, the photoelectrochemical synaptic device operates either in current mode (closed-circuit state) or in voltage mode (open-circuit state), allowing it to function in only one mode at a time. Essentially, these two modes are separated from each other and do not influence each other, thus not affecting synaptic weight updates. We introduce both current and voltage modes to highlight the difference between our device and those that only operate in current mode. Our device features dual-modal operation, offering the flexibility to select either current (STP) or voltage (LTP) mode according to the requirements. In our future research, we aim to leverage the CMOS-compatible and low-cost silicon platform, along with micro/nano-fabrication techniques, to develop large-scale photoelectrochemical synaptic device arrays. Additionally, tailored peripheral circuits will also be developed to accommodate the dual-signal characteristic of our device. Furthermore, we will explore more application scenarios that require devices with dual-modal synaptic properties or chemical sensitivity, thus leveraging our device to meet practical demands.

In the end, we would like to express our gratitude once again to all reviewers for raising critical comments to improve the quality of our manuscript. Hope our responses have addressed your concerns fully.

All authors.

REVIEWERS' COMMENTS

Reviewer #1 (Remarks to the Author):

The reviewer's concerns have been addressed.

Reviewer #3 (Remarks to the Author):

The authors have addressed the comments and I recommended its publication now.

Response letter

Reviewer #1:

Overall comment: The reviewer's concerns have been addressed.

[Overall response]

We sincerely appreciate the time and effort the reviewer has dedicated to improving the quality of our manuscript.

Reviewer #3:

Overall comment: The authors have addressed the comments and I recommended its publication now.

[Overall response]

We appreciate the reviewer's recommendation of our revised work. We also thank the reviewer for the time and effort spent during the review process.